Author reply to Referee comments from **Anonymous Referee # 1** from 19 November 2018 (https://doi.org/10.5194/essd-2018-98-RC1, 2018) on:

A long-term (2002 to 2017) record of closed-path and open-path eddy covariance CO_2 net ecosystem exchange fluxes from the Siberian Arctic

by David Holl et al.

Reviewer comments (RC)
Author comments (AC)
Manuscript changes (MC)
Please note that figure numbers in this document refer to figures in this document and not to the numbering in the original draft unless denoted otherwise.

RC 1

1.) Inclusion of a 'scientific overview' In the 'Site description' Section, the first 5 paragraphs give a comprehensive overview on the site conditions, while the last paragraph is clearly detached from this material, and in its present form does not belong there. Still, I believe it will be of use to the reader to demonstrate what has been found so far based on the flux time series presented in this manuscript. My recommendation is to move this paragraph to a new chapter 4, i.e. between methods and data availability, and extend it to a length of 3-4 paragraphs in total. This would give ample room to summarize the main findings based on Samoylov eddy-covariance (and other) data so far, therefore highlighting the value of the dataset presented herein, and the role of the site in general for Arctic climate change research.

I moved and extended the paragraphs about scientific findings from the "Site Description" section to a new chapter 5 "Scientific overview" before the conclusions as suggested. Please also note my reply to RC 4 below.

While results on methane exchange fluxes and the soils' methane production and oxidation potential are more prominent in the publication record (e.g. Wagner et al., 2003; Kutzbach et al., 2004; Liebner and Wagner, 2007; Knoblauch et al., 2008; Sachs et al., 2008; Wille et al., 2008; Schneider et al., 2009; Sachs et al., 2010; Liebner et al., 2011; Knoblauch et al., 2015), literature on CO_2 flux time series recorded with the same measurement system presented in this publication is available for distinct years. Flux processing has, however, been streamlined only now. The length of the time series, the addition of detailed footprint information, the site-specific correction of OP fluxes and the coherent processing and quality filtering distinguishes the data set at hand from past publications like the contribution made to the FLUXNET2015 data set (Kutzbach et al., 2015).

Ongoing analysis of the long-term data set (Kutzbach, unpublished) *inter alia* confirms what has been found in the past (Kutzbach, 2006; Kutzbach et al., 2007; Runkle et al., 2013). The polygonal tundra of Samoylov Island appears to be a robust growing season CO_2-C sink whereas this sink strength can vary that much interannually that prolonged low-level respiratory CO_2-C loss during the cold season can offset CO_2-C uptake during the vegetation period. Reduced summer uptake has been observed for both the coldest and warmest summers. Runkle et al. (2013) found that with frequent early season heat spells, the temperature-induced increase in respiratory release can exceed the rise in photosynthetic uptake. Recently, all data from this publication has been contributed to the Arctic Data Center's chamber and EC synthesis project *Reconciling historical and contemporary trends in terrestrial carbon exchange of the northern permafrost-zone* that aims at identifying seasonal and interannual C flux dynamics and its drivers based on a newly established pan-arctic data base.

In context with the improvement of earth system models (ESMs), carbon dioxide fluxes from Samylov Island can be especially of use due to the site's comparably high moss cover. Using data from Samoylov, Chadburn et al. (2017) found that current ESMs miss an observed early season CO_2 uptake peak suspected to be connected to the earlier onset of moss photosynthesis in comparison with vascular plants. Although there have been advances and e. g. Porada et al. (2013) developed a dynamic moss model for JSBACH (Raddatz et al., 2007), Chadburn et al. (2017) noted that the simulated CO_2 uptake and release terms combining vascular vegetation and moss carbon fluxes did not agree with observational data. The fact that the Samoylov Island NEE data set has now been extended and its quality has been greatly improved holds the opportunity to estimate the performance of updated ESM versions that are set up to represent carbon fluxes in the moss layer better.

RC 2

2.) Ensure that tower locations do not disrupt continuous time series The combination of text in Section 3.1, Figure 1 and Table 1 provides a good overview on the different site setups used to form this 16-year data record. However, the material also raises the question how the shifts in tower position and sensor configuration, including sensor height, may have influenced the signal captured by the EC system, and therefore maybe biased the long-term time series. I therefore recommend moving Section 3.6 upward as a new Section 3.2, and extending the discussion of the footprint issue. You can use parts of the conclusions section for this, but more details need to be provided how the shifts in landscape element fraction in the footprints may have compromised the continuity of the flux observations. See also my comment on Section 3.6 in the 'line comments' below.

I added a new "Discussion" section to the manuscript addressing the effects of tower location shifts and other possible disruptions of the time series' coherency.

Although we did our best to ensure the consistency and appropriateness of the data processing workflow for the presented NEE time series, due to technical and logistical constraints during 16 years of field work, disparities in the experimental setup exist which may challenge its integrity. The EC tower was relocated twice, the measurement height was changed three times (see Figure 1 and Table 1 *(in original draft)*). These changes of tower location and measurement height affected the source area and hence the surface types sampled during flux measurements. Most notably, between July 2007 and June 2009, the EC tower was placed about 650 m south-west of its original position at the center of Samoylov Island, in an area with an increased coverage of the surface class wet tundra. This is revealed by the footprint analysis (Figure 1). While the EC footprint is dominated by the surface class *dry tundra* throughout the time series, during subperiods 2007, 2008 and 2009 I the contributions of *wet tundra* to the measured flux are significantly higher.

To check the effect of the shifts in tower location and measurement height on cumulative CO_2-C fluxes, we calculated flux sums for a period when flux time series without gaps were available in most years. The overlapping period covers days of year 200 to 234, i.e. part of the growing season in all years except for 2004 (see Figure 2). Interannual variability of cumulative C fluxes in years with constant tower location (and measurement height) appears to be large and driven by a more complex set of variables than shifts in surface class contributions only. Flux sums from the periods when EC tower relocation led to a significant shift in EC footprint composition are well within the range of the distribution of cumulated fluxes from years with a more homogeneous EC fetch area. We therefore assume that, at least with respect to budget calculations, the presented long-term time series is not disrupted and can be regarded as representative for a polygonal tundra site dominated by dry tundra. For a more in depth analysis of flux dynamics, footprint information should and can be considered by users of the data set. Recently, a comparison between surface class level NEE models based on chamber measurements with EC fluxes, using the half-hourly footprint information provided in this data set for scaling, yielded good agreement between the results obtained with both methods Eckhardt et al. (2018). We regard the availability of half-hourly footprint information in the presented NEE data set an attribute that sets it apart from other studies and holds chances for comprehensive analyses.

Apart from the changes in anemometer height, other deviations of the general instrument setup occurred due to limitations in data storage during two winter periods when the acquisition frequency was reduced to 5 Hz and 10 Hz respectively. Rinne et al. (2008) demonstrated in a field experiment that fluxes calculated from raw data recorded at frequencies below 20 Hz compare well with fluxes derived from high frequency raw data. Differences arise as an increase of random noise and not as a systematic bias. High frequency noise removal before ensemble spectra estimation in EddyPro is effective in limiting the effect of increased noise on the quality of transfer function estimation in the process of spectral correction. Overall spectral correction in EddyPro is expressed as a spectral correction factor SCF which comprises the effect of all applied compensations for high and low frequency loss. Raw fluxes are multiplied with the respective SCFs during processing. We compared the SCF distributions of the two above mentioned winter periods with statistics of the remaining parts of the time series when data was recorded at 20 Hz. SCF deviations between the different acquisition frequencies are minor (see Figure 03) implying that systematic differences between fluxes calculated form raw data of different temporal resolutions are in fact small, random uncertainties increase, however.

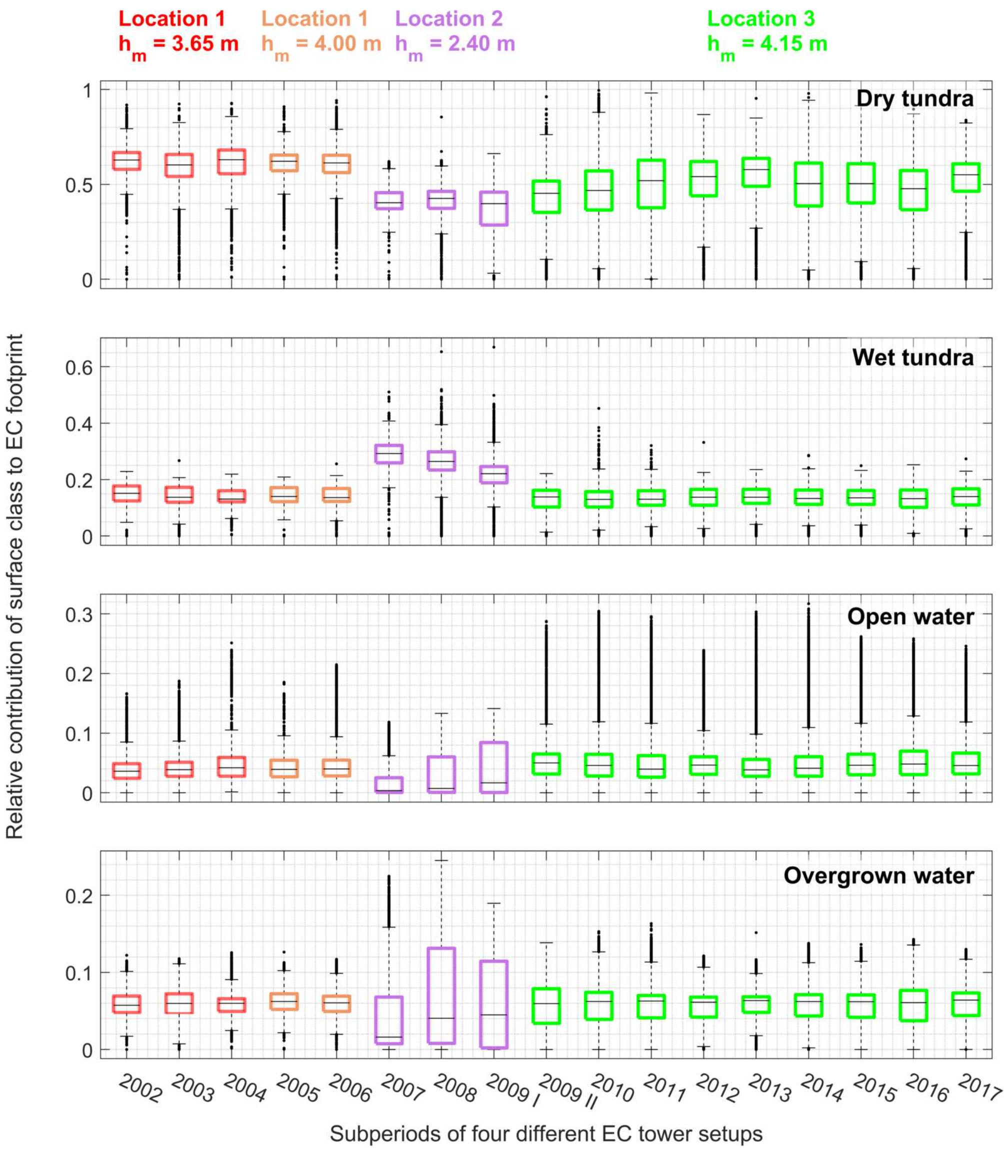

Fig. 1 Mean surface class composition of the eddy covariance footprint during 17 subperiods of four different tower setups at three locations on Samoylov Island.

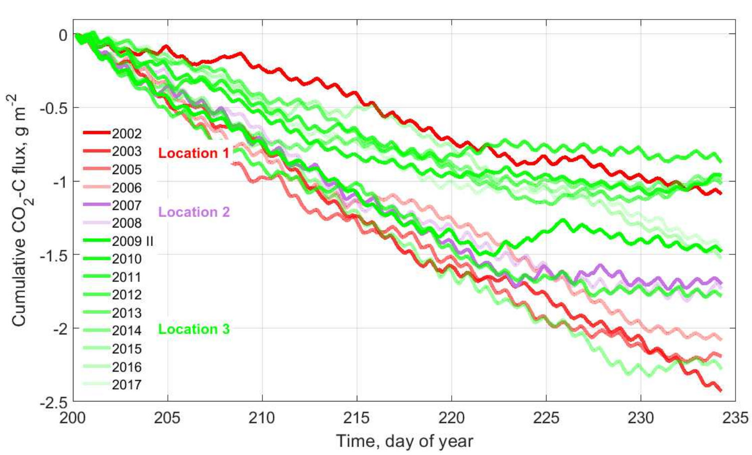

Fig. 2 Comparison of cumulative CO_2 flux sums of different years during the same day of year range.

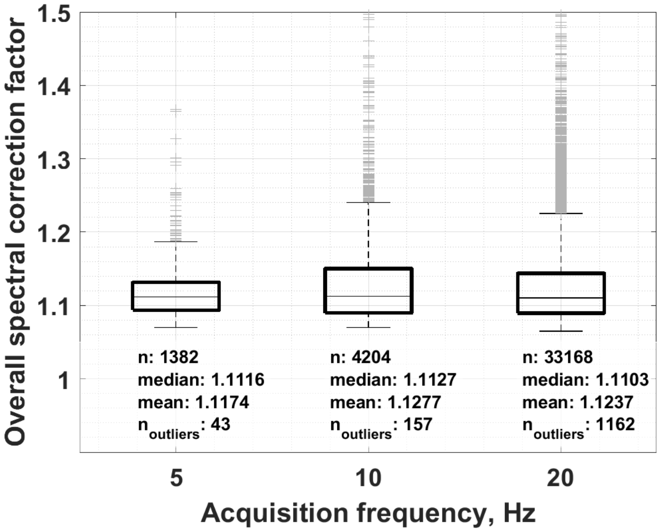

Fig. 3 Spectral correction factor statistics for periods with different acquisition frequencies.

RC 3

3.) Flux uncertainty description, and discussion A clear definition of data uncertainty is mandatory for publications in this journal. In Section 3.2, you briefly mention that you used the standard EddyPro feature to estimate random flux uncertainties – which is a good start, but certainly deserves more attention. So please work out in a separate paragraph what these random uncertainties consist of, and how exactly those were addressed in EddyPro. Moreover, there are also potential sources of systematic uncertainties in eddy covariance flux measurements, e.g. data-processing errors, or instrument calibration issues. These should ideally be covered directly in your uncertainty assessment of the flux data. Since you obviously decided to ignore them here, you should at least provide a convincing rationale why this simplification is justified.

I added a new part "Flux uncertainty estimation" to the "Methods" section.

Flux uncertainty can be regarded as a combination of a systematic and a random part. While the attempt should be made to remove systematic biases, random errors cannot be corrected for Richardson et al. (2012). However, statistical methods exist to estimate the uncertainty of a flux measurement due to random errors. We used three different approaches from literature to quantify random uncertainty and addressed fluxes with a suspected large bias by correcting for it during processing or by filtering in the course of quality assessment.

Most importantly, systematic errors are introduced when underlying EC assumptions are not met. Using the method of Mauder and Foken (2004) that combines an assessment of well developed turbulence and steady state conditions, we identified biased fluxes and flagged them. Other sources of systematic errors that we addressed include for example the angle of attack correction of faulty sonic anemometer readings, filtering for low instrument signal strength, the OP self-heating correction and compensations for high frequency loss and air density fluctuations (see sections 3.2.2, 3.3 and 3.4). Although we are confident that we applied corrections for systematic errors both rigorously and carefully enough, biases were certainly not always removed entirely. The quality flags included in the data set, reflect a level of confidence based on the assessment of general EC assumptions and our six additional quality filtering steps (see section 3.3).

To be able to include a random uncertainty estimate for each individual OP and CP flux in the provided data set, we set EddyPro to calculate random uncertainty estimates following Finkelstein and Sims (2001). The authors developed a method that aims at quantifying flux uncertainty associated with turbulence sampling errors. These errors can contribute largely to the total random error as they refer to the insufficient sampling of large eddies with high spectral energy. Due to the stochastic nature of turbulence, this type of error is random. To estimate its magnitude, the so-called integral turbulence timescale (ITS) is first determined by expressing the covariance of vertical wind velocity and gas concentration as a function of a lag time between these two time series. The ITS is then given by integrating the cross-correlation function theoretically from 0 to infinity, in practice, however, until an upper lag time limit is reached. The upper limit can be defined in three different ways in EddyPro. We used the definition of the normalized cross-correlation function reaching a value of 1/*e* = 0.369 to determine an upper lag time limit used for integration. While the normalized cross-correlation should reach zero with increasing lag time in theory, in practice it sometimes does not. The setting we used on the one hand provides the least conservative estimate of the ITS but on the other hand offers computational efficiency and makes sure that an upper limit for integration can reliably be found. With the ITS, a flux uncertainty can be determined by calculating the variance of an EC flux or, as Finkelstein and Sims (2001) put it, by calculating the variance of the covariance. This ensemble variance would approach zero with the averaging time approaching infinity. In the data set available for download, a random uncertainty estimate calculated with the method of Finkelstein and Sims (2001) is given for each OP and CP flux (see Table 6 in original draft). Random uncertainties based on ITS estimation observations increase with absolute fluxes with mean values of 0.16 and 0.05 µmol m^{-2} s^{-1} for OP and CP fluxes (see Figure 4). OP random uncertainty estimates are generally larger and more scattered with respect to the corresponding flux values.

As the above described random uncertainty estimate specifically addresses the turbulence sampling error, other sources of random flux errors such as the noise introduced by the different components of the measurement system are neglected. With simultaneous measurements from two sensors, we could additionally estimate random errors for the measurement system as a whole during times when the data sets from both sensors overlapped. We followed the paired observations approach as presented by Dragoni et al. (2007) and calculated a random error estimate ε as

$$\epsilon = \frac{1}{\sqrt{2}} \cdot (F_{CP} - F_{OP})$$

with the closed-path and open-path CO_2 fluxes F_{CP} and F_{OP} of quality classes 0 and 1 in µmol m^{-2} s^{-1}. The distribution of ε estimates is shown in Figure 5. The ε values calculated with OP fluxes corrected for the self-heating error have a mean close to zero and are distributed more symmetrically than the ε values calculated with uncorrected OP fluxes. The mean of this distribution is shifted from its mode as well as from zero, indicating a much stronger systematic component whithin the measurement error. This result increases our confidence that the OP self-heating correction we applied was successful in removing a systematic bias from the data.
Further following Dragoni et al. (2007), we used the ε system error data set from the overlap period to generate flux uncertainty estimates for bins of increasing OP flux ranges. We sorted the ε values in 20 corresponding flux bins between -2 and 2 µmol m^{-2} s^{-1} and calculated an uncertainty estimate for each bin $\sigma(\varepsilon)_i$ as

$$\sigma(\epsilon)_i = \sqrt{2}\frac{1}{N_j}\sum_{j=0}^{N_j} |\epsilon_{i,j} - \overline{\epsilon}_i|$$

Results show (see Figure 4) a similar data range and pattern of uncertainty estimates in relation to associated fluxes like the half-hourly values calculated after Finkelstein and Sims (2001).
As a third method of random uncertainty estimation we simplified the successive observations approach from Richardson et al. (2006) by using results of the quality run performed during MDS gap filling (see section 3.5). We selected the time steps when an flux observation and a MDS value that was estimated using a one day window and the MDV technique were available. We used the standard deviation of the fluxes measured at the same hour of day within a one day window, as an uncertainty estimate of the observed flux. Results are shown in Figure 4 and also increase with rising absolute fluxes in the same ranges as random uncertainties due to turbulence sampling error or measurement system error do.
We included the results obtained with ITS estimation into the uploaded data set considering the similarity between the uncertainty-flux relations calculated with independent methods as well as due to the advantage of a distinct uncertainty estimate for each sensor and time step.

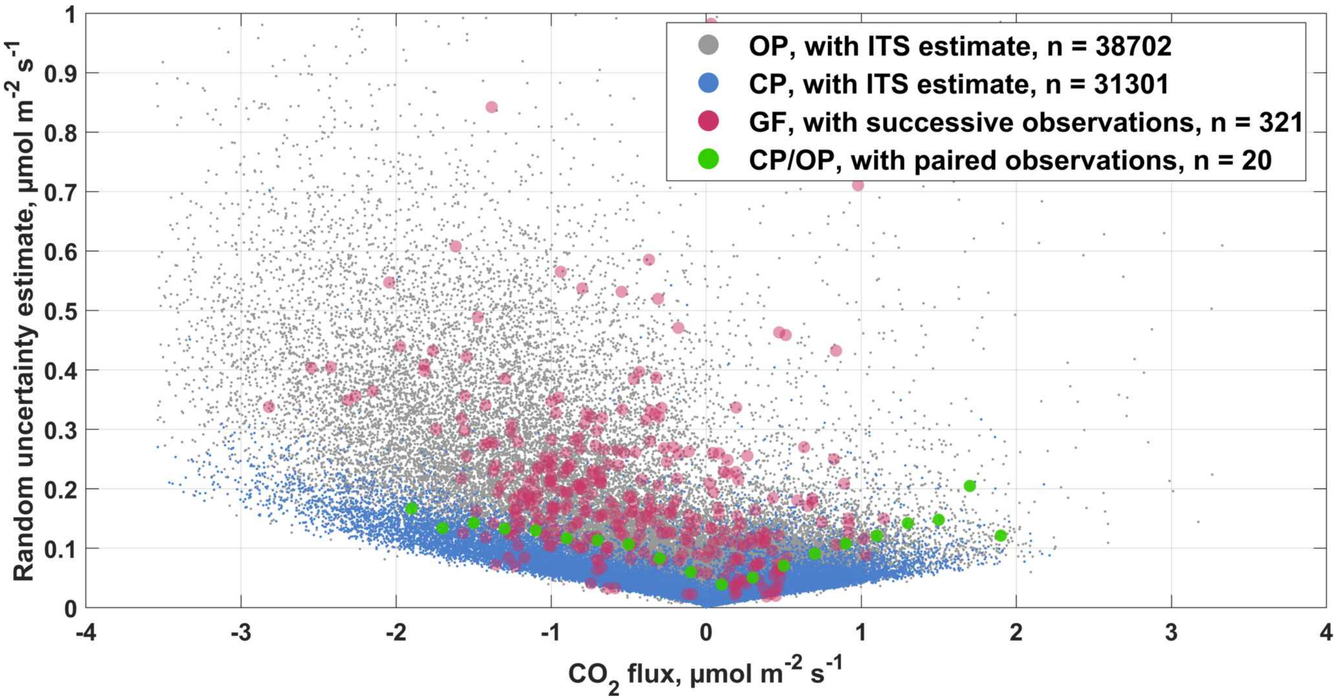

Fig. 4 Random uncertainty estimates for all closed path (CP) and open-path (OP) CO2 fluxes calculated using (1) estimates of the integral turbulence time scale (ITS), (2) the successive observations approach and results from gap filling (GF) and (3) the paired observations approach during periods with simultaneous OP and CP records.

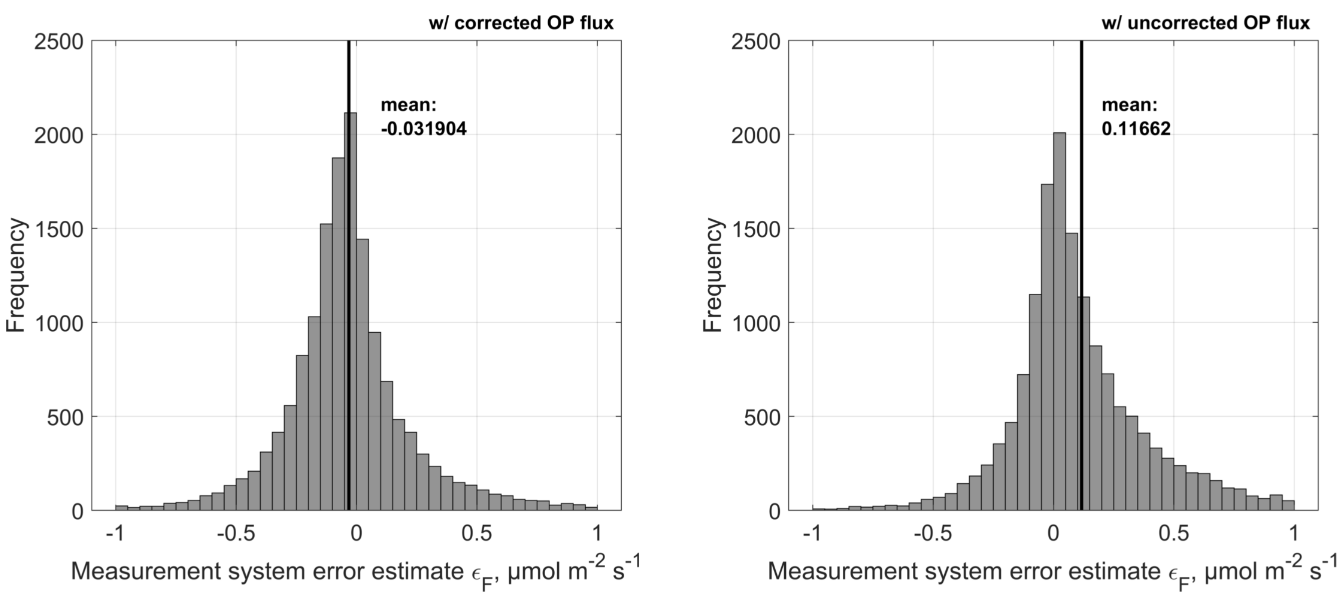

Fig. 5 Distributions of the measurement system errors ε estimated using the paired observations approch for differences between closed path and corrected (left panel) as well as uncorrected (right panel) open-path (OP) fluxes.

Line comments:

RC 4

p.1, abstract & introduction: Within these sections, I'm missing data-driven insights. Having a 16-year data record at hand, I would first think about analyzing the data directly to determine long-term trends in surface-atmosphere exchange processes. Next, I would aim at generating process insights, e.g. what causes interannual and inter-seasonal variability in flux rates, Only then I would start thinking about the time series being a useful resource for calibrating and validating process models. I think these data-driven topics deserve additional attention in both sections.

We regard this dataset publication as a starting point for analysis of flux dynamics done by us and other members of the scientific community. We are aiming at publishing those types of results in the future (Kutzbach, unpublished). In this paper, however, we wanted to focus on the methods we used to process the data rather than its interpretation. To our understanding, this proceeding is in line with the "Aims and scope" of ESSD, which is one reason why we selected this journal.

"Articles in the data section may pertain to the planning, instrumentation, and execution of experiments or collection of data. Any interpretation of data is outside the scope of regular articles. Articles on methods describe nontrivial statistical and other methods employed (e.g. to filter, normalize, or convert raw data to primary published data) as well as nontrivial instrumentation or operational methods. Any comparison to other methods is beyond the scope of regular articles." (https://www.earth-system-science-data.net/about/aims_and_scope.html)

RC 5

p.1, l.6: FLUXNET is not restricted to CO2 fluxes

True, this is a lapse. I changed "The site is part of the international network of carbon dioxide flux observation stations (FLUXNET, Site ID: Ru-Sam)." to

The site is part of the international network of eddy covariance flux observation stations (FLUXNET, Site ID: Ru-Sam).

RC 6

p.2, l.7: excessive use of references for a single statement

I do not agree. The reference list is meant to express that many authors agree on the importance of permafrost carbon pools in the context of climate change. The references are thought to proof the statement of "wide recognition" of the topic.

RC 7

p.2, l.16: not sure what inversion model have to do with the scope of this paper. They are trained on mixing ratio observations, not fluxes.

Thank you for pointing out this fact. I changed the sentence to:

McGuire et al. (2012) conclude that reducing uncertainties of regional estimates based on observational data relies on high quality ground-based measurements that should be placed strategically, e. g. along hydrological or vegetation gradients.

RC 8

p.2, l.30f: this section could use a map to show location of the delta, and the island itself

I added an overview map (Figure 6 in this document).

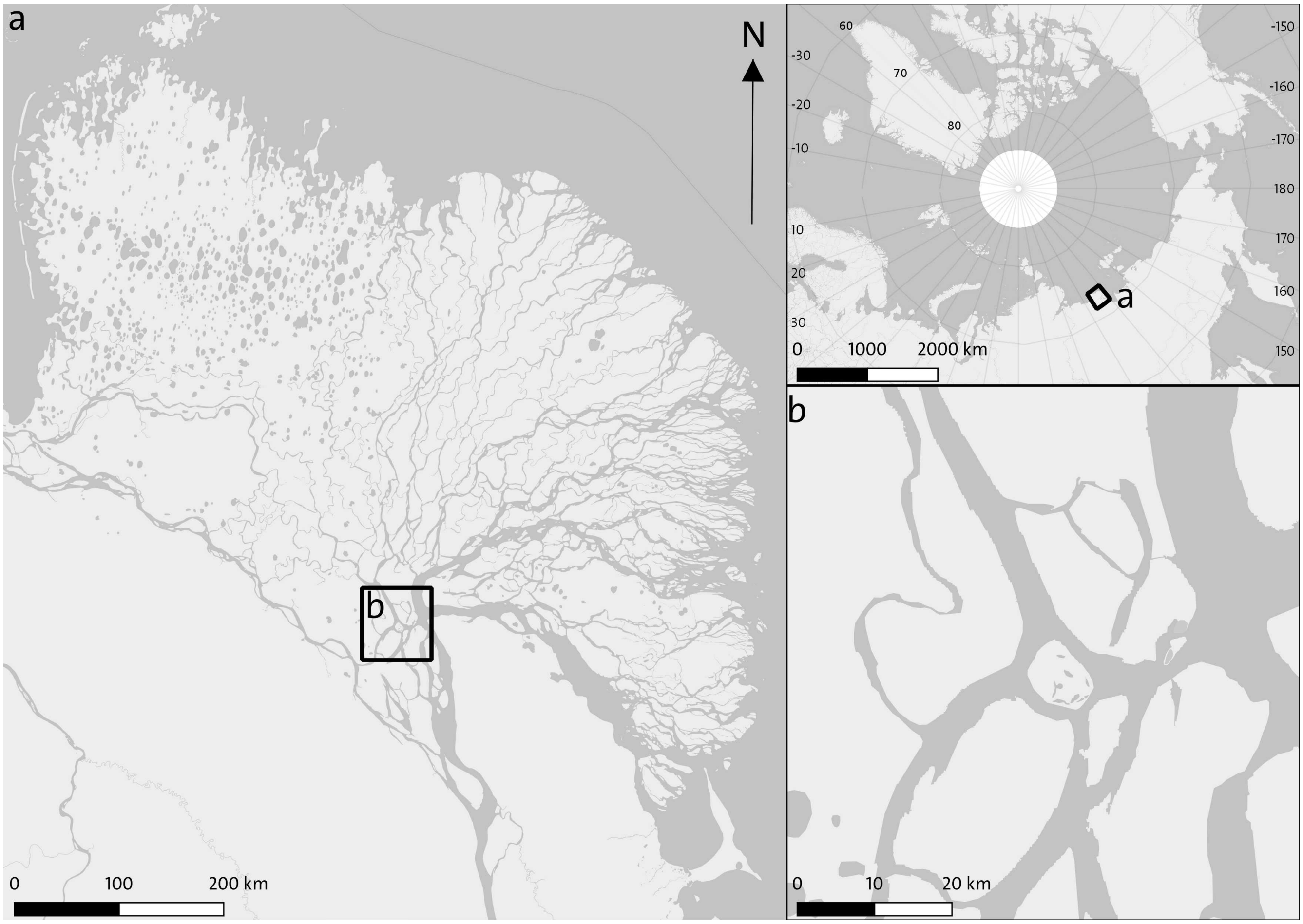

Fig. 6 Location of Samoylov Island (center of panel b) in the Lena River Delta (panel a). Map data from: OpenStreetMap contributors, under Open Database License

RC 9

p.3, l.17: there is no high-centered polygon on the entire island ..??

Yes, there are some high-centered polygons on Samoylov. I changed the sentence.

In contrast to the modern floodplain, the river terrace's surface is patterned due to frost-action that formed a wet polygonal tundra landscape consisting of mostly low-centered and some high-centered ice-wedge polygons as well as thermokarst lakes and channels.

RC 10

p.3, l.29ff: climatology information given here is certainly useful, but only based on a #20 year record from the site itself. It may be helpful to compare to longer-term climate records from the region (e.g., for Tiksi there is data starting in the 1930s).

I agree, I added longer-term meteorological information from Tiksi.

The closest WMO (World Meteorological Organisation) weather station is located on the continent, around 110 km southeast from Samoylov Island in the city of Tiksi. Between 1936 and 2017 the mean air temperature reported from Tiksi is – 12.74 °C, mean annual precipitation amounts to 304.5 mm (AARI, 2018). While the mean air temperature in Tiksi is very similar to the 20-year mean from Samoylov Island, average annual precipitation appears to be much higher in Tiksi than in the delta region. Boike et al. (2013) explain this divergence with the fact that Tiksi is located at the coast of the Laptev sea and surrounded by mountains.

RC 11

p.4, l.1f: is there any record of snow depth, and its variability?

I added information on snow depth from Boike et al. (2018).

..., the snow-free periond 138 ± 18 days. Snow depth was reported by Boike et al. (2018) averaging 0.3 m between 2002 and 2017 with a maximum of 0.8 m in 2017. Beginning in early to mid-June,...

RC 12

p.5, l.6ff: you may add the power consumption as another important difference between CP and OP systems.

I added a remark on power consumption to the sentence starting in line 11 of page 5.

OP sensors are commonly installed in close proximity to the anemometer and do not require a pump that greatly reduces the power consumption of OP instruments compared to CP setups.

RC 13

p.6, l.4ff: even though you spend a few sentences to describe the WPL-approach, you fail to mention that this is about accounting for the influence of density fluctuations

I agree, the WPL-approach needs a more thorough and clear introduction. I therefore rewrote the section from page 5, line 14 (starting with "CP analyzers have the...") until page 6, line 8 (before "Major drawbacks...") and moved it to a new paragraph.

Infrared gas analyzers typically measure gas densities and report the number of molecules per volume of air. To be able to refer the mass of a gas to the mass of air, gas densities are transformed to mixing ratios using air density. However, as the optical path of an OP gas analyzer is exposed to the varying temperature, pressure and humidity conditions of the atmosphere, air density in the measurement cell fluctuates mainly due to thermal expansion/contraction and water dilution/concentration. This effect, that leads to faulty concentration readings of OP instruments and thereby to incorrect flux estimates, has first been described by Webb et al. (1980). The authors proposed two flux correction terms to compensate for these density fluctuation effects that are referred to as Webb-Pearman-Leuning (WPL) terms and have since been verified experimentally and theoretically and are routinely applied in OP EC studies. Especially at times of low gas fluxes, WPL terms can become orders of magnitude larger than raw gas fluxes (Munger et al., 2012). CP analyzers have the advantage of controlled temperature and pressure conditions in the measurement cell, allowing for the sample-wise calculation of mixing ratios rather than molar densities (Ibrom et al., 2007b) and thereby avoiding the need to apply air density fluctuation correction terms after raw flux calculation.

RC 14

p.7, Section 3.3: It's a bit odd that you start describing some elements of quality flagging already in Section 3.2, and continue with this material here, in the main quality section. This should be cleaned up. Also, you fail to reference Table 3 in the text. Moreover, you should improve the structure of this Section. You begin with a too short general overview on additional quality filters, and how they are used in the overall QC flagging scheme. You then close the section with very similar statements. This should be merged to a single introductory paragraph that clearly states that you applied 6 more quality checks, and if any of them indicated problems, the quality flag was set to 2.

Thank you for the suggestion, I agree, the "Quality filtering" section (3.3) should be more clear. I moved the end of section 3.2 (from page 7 line 21 to the end of the paragraph) to a newly formulated introduction of section 3.3. As suggested, I also moved the end of section 3.3 (page 8, line 23, starting from "In the dataset available...") into this new introductory paragraph. Section 3.3 now begins with:

We set EddyPro to calculate quality flags according to Mauder and Foken (2004) that represent flux quality in three classes (0, 1 and 2) with 0 denoting the highest and 2 denoting the lowest quality class. This quality evaluation is based on tests for stationarity and developed turbulence and thereby indicates whether general EC assumptions about atmospheric conditions were met during a flux calculation period. Flux quality assessment was largely based on the scheme of Mauder and Foken (2004). In the data set available for download, we included one column for each analyzer type containing this quality flag. Additionally, we applied six further screening steps and flagged fluxes of low quality. If a flagged flux was not already assigned to class 2 according to Mauder and Foken (2004), we set the quality flag to 2. Fluxes of quality class 2 should be omitted from further analysis. They are included in the reported dataset for the sake of completeness. We performed the six additional flagging steps in the following sequence. An overview of these filtering steps including the number of flagged values is given in Table 3 (*in original draft*).

RC 15
p.8, l.14: The choice of 450ppm as the upper concentration limit seems rather narrow. Can you please justify?
I want to stress that this limit refers to half-hourly average concentrations, the absoute concentration filter applied to the high frequency data during raw data screening in EddyPro (following Vickers & Mahrt, 1997) allowed a much wider range (200 ppm to 900 ppm) of concentrations. The limit of half-hourly average concentrations was decided for after calculating the 95th percentile of closed-path (440 ppm) and open-path (410 ppm) averages for timesteps with flux qualities 0 and 1.

RC 16
p.9, Fig.2: Figure 2 isn't really informative, since it's hard to distinguish between corrected and uncorrected time series in such a cloud of values. Please think about a different format (box plots?), or just leave out the plots, and show the regression statistics instead in a table.
I replaced the figure and added a table with the regression statistics.

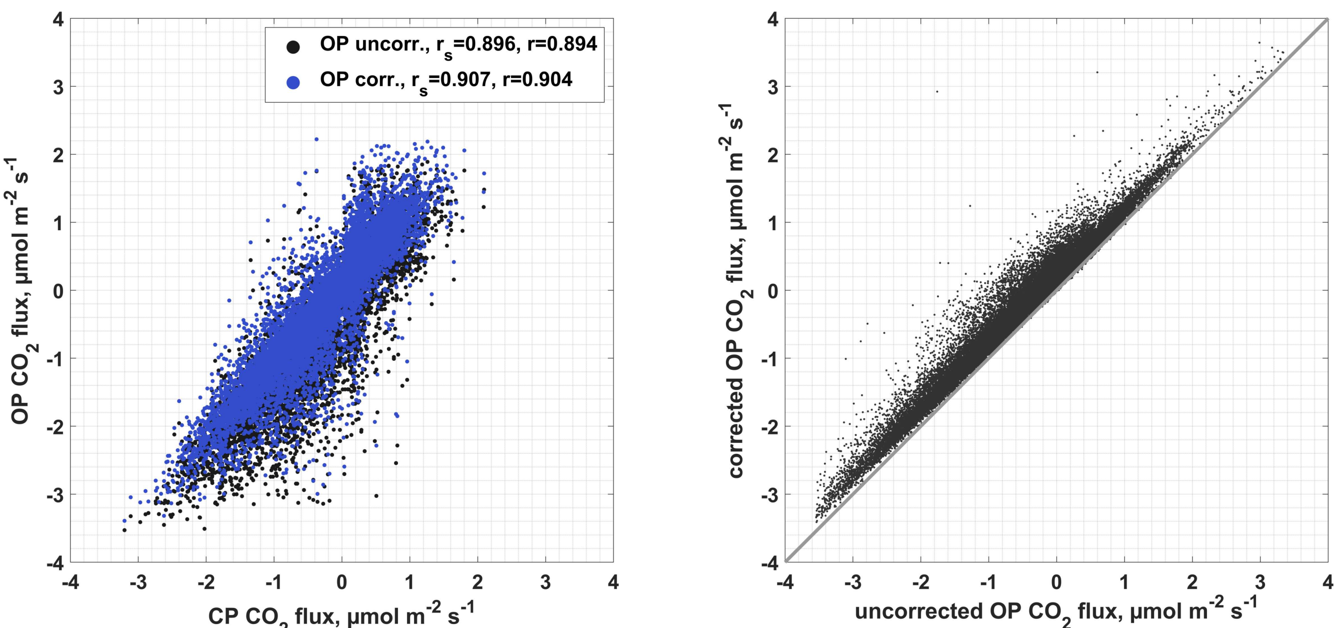

Fig. 7 Effect of the self-heating correction on the correlation between open-path (OP) and closed-path (CP) fluxes (left panel). Only quality class 0 is shown. Negative fluxes are affected more strongly by the correction than positive fluxes (right panel).

Table 1 Spearman's rank correlation coefficient rs and Pearson's correlation coefficient r between closed-path (CP) and open-path (OP) fluxes with and without the applied self-heating correction. The agreement between CP and OP fluxes increases throughout all quality classes after OP correction.

		Quality class 0	Quality classes 0,1	Quality classes 0, 1, 2
r_s	OP uncorrected	0.896	0.866	0.508
	OP corrected	0.907	0.871	0.512
r	OP uncorrected	0.894	0.871	0.042
	OP corrected	0.904	0.877	0.055

RC 17
p.10, Section 3.5: I suppose Figs. 3 & 4 should belong to this section. They are not referred to in the text. Moreover, it's not necessary to show Fig.4, since given the minor absolute shifts in fluxes after Burba correction in this case, the differences between figures are not discernible. As an alternative for Fig.4, it may be interesting to show the gap-filled time series, maybe even in cumulative form?
I agree, the gain of information from Figures 3 and 4 in the original draft is limited. I replaced both with one new Figure (Fig. 2 in this document) showing the measured time series that we compiled from open-path and closed-path records as well as the gap-filled time series.

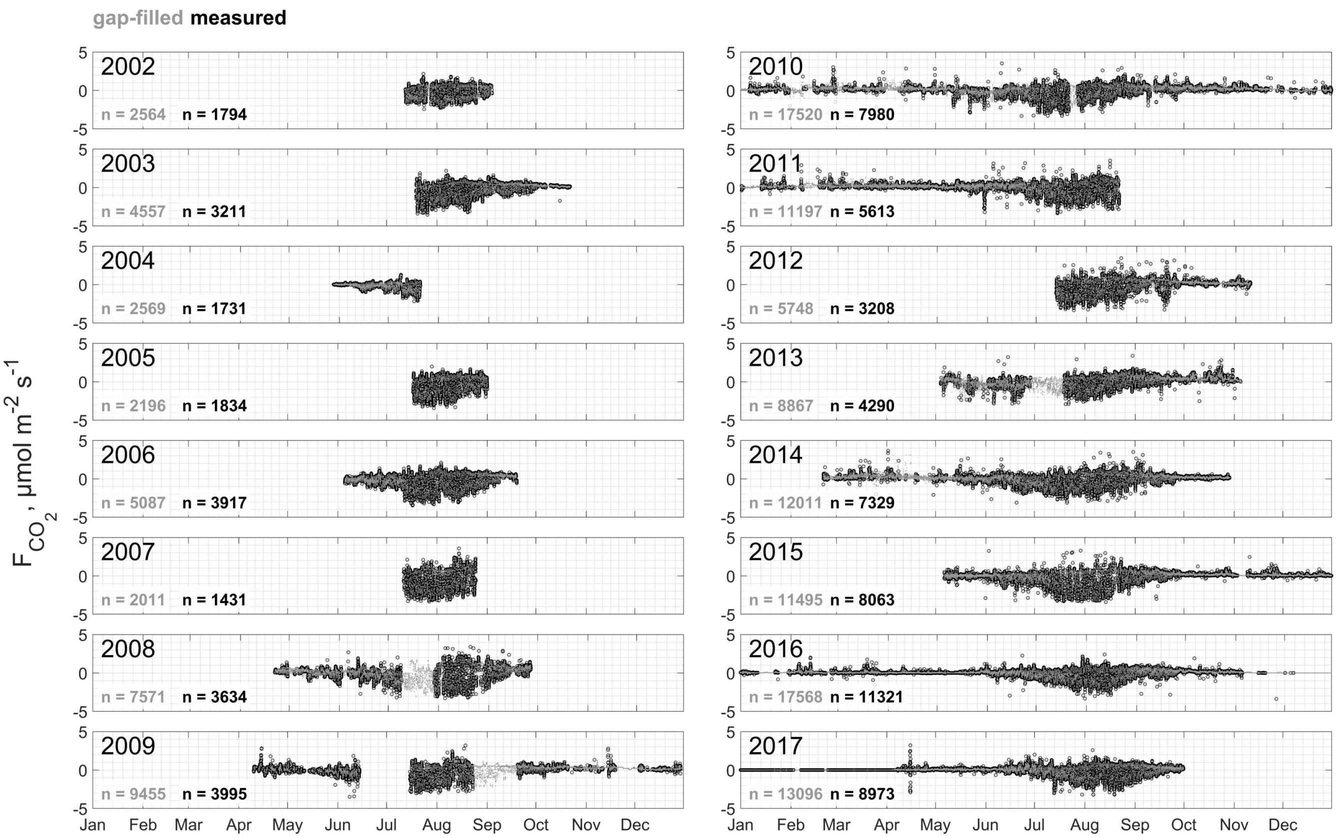

Fig. 8 Multiannual carbon dioxide flux time series compiled from fluxes measured with closed-path and open-path sensors on Samoylov Island's river terrace. Fluxes of quality class 2 are not shown. Self-heating errors in the OP data set have been corrected for. Additionally, the result from gap filling this time series with the MDS method is shown. The given numbers of values for the gap-filled time series include measured fluxes.

RC 18
p.11, Section 3.6: while the method applied to calculate footprints is sufficiently detailed, it is not fully clear how footprint results were combined with the land cover map. What's completely missing here is a reference to the findings, a.k.a. a bottom line. As already mentioned in the 'medium comments' above, this is an important piece of information, since (as shown in Table 1) multiple positions with multiple sensor heights were used over the 16 year data record. The authors clearly need to point out that this mixture of setups is still suitable to form a coherent, long-term time series of flux exchange for this site. It's not sufficient to just briefly mention these results in the conclusions. In particular, the results in Table 5 emphasize that the southernmost tower position, used within the years 2007-2009, featured a quite different composition of landscape elements than the northern site position. The authors need to make an effort to convince the readers that these differences did not result in a significant deviation of flux patterns, and therefore would bias the long-term trends.
I added a new "Discussion" section detailing the effects of tower relocations. See my response to RC 2 above.

I added more information on how the footprint results were combined with the land cover map to the end of section "Footprint modeling"

...We evaluated the footprint model at the same resolution that was used by Muster et al. (2012) to classify the surface (i. e. 0.14 m x 0.14 m). We could thereafter assign a probability of being the EC source area to each classified pixel and sum up the probabilities of all pixels belonging to the same surface class to estimate the contribution of each class. This proceeding to combine an EC source area estimation with a land cover classification is similar to what has been applied and described in more detail by Forbrich et al. (2011).

RC 19

p.11, Section 4: It's good to list the parameters given in the PANGAEA dataset in a separate table. However, since this dataset is obviously restricted to CO2 fluxes and their QC parameters, it would be good to also list the source for ancillary meteorological information, if available, since those will be necessary to put the flux time series into contex

I added a reference to ancillary measurements to the "Data availability section.

Ancillary long-term time series of meteorological and soil variables from Samoylov Island are available from Boike et al. (2018) and can be accessed through https://doi.pangaea.de/10.1594/PANGAEA.891142

I also added a new paragraph to the conclusions pointing out the importance of these ancillary data.

Furthermore, analysis of this NEE time series is not limited to the gas flux data only. An extensive data stream of meteorological and soil variables between 2002 and 2017 has recently been published by Boike et al. (2018). The authors made their records publicly accessible on the two long-term repositories Pangaea (https://doi.pangaea.de/10.1594/PANGAEA.891142) and Zenodo (https://zenodo.org/record/2223709). The fact of parallelly available ancillary ecosystem variables enables a potential user to put the gas flux dynamics reported in this publication into context with the variability of other ecosystem properties and potential flux drivers. We regard this type of analysis as vital to understand inter-annual variability of CO2 fluxes on Samoylov Island and are working on it ourselves (Kutzbach, unpublished).

New References

Chadburn, S. E., Krinner, G., Porada, P., Bartsch, A., Beer, C., Belelli Marchesini, L., Boike, J., Ekici, A., Elberling, B., Friborg, T., Hugelius, G., Johansson, M., Kuhry, P., Kutzbach, L., Langer, M., Lund, M., Parmentier, F.-J. W., Peng, S., Van Huissteden, K., Wang, T., Westermann, S., Zhu, D., and Burke, E. J.: Carbon stocks and fluxes in the high latitudes: using site-level data to evaluate Earth system models, Biogeosciences, 14, 5143–5169, 2017.

Eckhardt, T., Knoblauch, C., Kutzbach, L., Simpson, G., Abakumov, E., and Pfeiffer, E.-M.: Partitioning CO2 net ecosystem exchange fluxes on the microsite scale in the Lena River Delta, Siberia, Biogeosciences Discussions, 2018, 1–27, 2018.

Porada, P., Weber, B., Elbert, W., Pöschl, U., and Kleidon, A.: Estimating global carbon uptake by lichens and bryophytes with a processbased model, Biogeosciences, 10, 6989–7033, 2013.

Raddatz, T., Reick, C., Knorr, W., Kattge, J., Roeckner, E., Schnur, R., Schnitzler, K.-G., Wetzel, P., and Jungclaus, J.: Will the tropical land biosphere dominate the climate–carbon cycle feedback during the twenty-first century?, Climate Dynamics, 29, 565–574, 2007.

Richardson, A. D., Aubinet, M., Barr, A. G., Hollinger, D. Y., Ibrom, A., Lasslop, G., and Reichstein, M.: Uncertainty quantification, in: Eddy Covariance: A Practical Guide to Measurement and Data Analysis, edited by Aubinet, M., Vesala, T., and Papale, D., pp. 173–209, Springer, 2012.

Richardson, A. D., Hollinger, D. Y., Burba, G. G., Davis, K. J., Flanagan, L. B., Katul, G. G., Munger, J. W., Ricciuto, D. M., Stoy, P. C., Suyker, A. E., et al.: A multi-site analysis of random error in tower-based measurements of carbon and energy fluxes, Agricultural and Forest Meteorology, 136, 1–18, 2006.

Rinne, J., Douffet, T., Prigent, Y., and Durand, P.: Field comparison of disjunct and conventional eddy covariance techniques for trace gas flux measurements, Environmental pollution, 152, 630–635, 2008.

Dragoni, D., Schmid, H. P., Grimmond, C. S. B., and Loescher, H. W.: Uncertainty of annual net ecosystem productivity estimated using eddy covariance flux measurements, Journal of Geophysical Research: Atmospheres, 112, 2007.

Author reply to Referee comments from **Anonymous Refferee # 2** from 29 November 2018 (https://doi.org/10.5194/essd-2018-98-RC2, 2018) on:

A long-term (2002 to 2017) record of closed-path and open-path eddy covariance CO_2 net ecosystem exchange fluxes from the Siberian Arctic
by David Holl et al.

Reviewer comments (RC)
Author comments (AC)
Manuscript changes (MC)
Please note that figure numbers in this document refer to figures in this document and not to the numbering in the original draft unless denoted otherwise.

RC 1
Review ESSD-2018-98 Siberian Permafrost
A login barrier on Pangaea prevents me from downloading the actual .tsv files. As it turns out I have a valid Pangaea login but, once in, I still cannot access the data. THIS VIOLATES ESSD POLICIES AND PREVENT ME OR ANY OTHER USER FROM FULL EVALUATION OF THE DATA!! This must be fixed immediately. All my comments below assume a quality effort on the part of the authors but until the data becomes fully and freely accessible, I must withhold approval of this manuscript.
The dataset is now accessible without limitations (https://doi.pangaea.de/10.1594/PANGAEA.892751). I addressed this issue with a short comment during the interactive discussion (SC1: 'Data access', David Holl, 14 Dec 2018).

RC 2
Page 3 line 15: this sentence should refer to eddy covariance "systems" because more than one instrument type was deployed on three different towers at two different locations.
I agree, "system" was changed to "systems".

RC 3
Page 3 line 30: technically, "low evaporation rates" should lead to dryer than expected atmospheric humidities. Perhaps the authors refer here to soil (moisture) conditions or to a combination of low specific atmospheric water vapour contents with lower temperatures that lead to a relatively high relative humidity?
The point we wanted to make here is that even though water input by precipitation is not very high on an annual basis, water loss by evaporation is even smaller. We failed to mention that low evaporation is indeed connected to low ambient temperatures and low water vapour pressure deficits.
I changed the sentence to:
An arctic-continental climate with low mean annual temperatures prevails in the Lena River Delta. Although precipitation is low as well, the climate can be considered humid as evaporation rates are low due to low ambient temperatures and relative humidity is high.

RC 4
Page 4, soils: much higher resolution soil mapping documented here than in the northern circumpolar soil atlas (Jones et al. 2010) so I understand better details here. But Jones et al. soil atlas, at least for central Siberia, adopts the "Russian Soil Classification System" while this paragraph references US or FAO definitions. Why? Because permafrost carbon estimates (e.g. Hugelius et al. in ESSD 2013, not cited here but used extensively in Koven and Schuur, both of which these authors do cite) depend substantially and in fact influence soil type classifications (e.g. again see Hugelius) in permafrost regions, this paper should at least document consistency with other soil classification systems? I know this is not a description of Samoylov permafrost soils data set, but we should at least know consistency or valid reasons for inconsistencies between soil classifications systems used by flux vs soil carbon communities?

The “Site description” section collects data that has been reported from Samoylov in the past. To my knowledge, Jones et al. 2010 do in fact use the FAO WRB system for soil classification. Unfortunately, Pfeiffer and Grigoriev (2002) and Zubrzycki et al. (2013) used a different classification. Hugelius et al. 2014 (“Estimated stocks of circumpolar permafrost carbon with quantified uncertainty ranges and identified data gaps“, Biogeosciences) did use SOC data provided by Zubrzycki et al. (2013) and therefore appear to regard this dataset as consistent with the methods and resulting estimates from other authors.

RC 5
Page 4 line 20 “contributied”
I corrected this typo.

RC 6
Page 4 line 25 (and following): “wind speed” I think you actually mean wind velocity because, unlike speed, you need both magnitude and direction?
I agree. I replaced “wind speed” with “wind velocity” at the appropriate places.

RC 7
Page 4 line 28: Need to mention here that, for a period of two years, the tower location moved almost 1 km to the west-southwest?
I think this fact is already made clear by saying “three different tower structures” and referring to Figure 1 (*in the original draft*) where the different locations are illustrated. The impacts of tower relocation are disscussed in more depth than in the original manuscript in a newly added “Disscussion” section. See my reply to RC 14.

RC 8
Page 4 line 30: For one year sampling rate went to 10 Hz, and later for a period of roughly 9 months sampling went to 5 Hz. Opportunity to test sampling and influence on spectral properties of flux calculations?
I agree, we missed the opportunity to report the impact of changing sampling frequencies on the spectral properties of the raw data. I added a new Discussion section to the manuscript where this topic is addressed. See my reply to RC 14.

RC 9
Page 5 line 2: “... the data set contains year-round fluxes in some years ...”. But, from Figure 3, only 2016 had anything close to full annual coverage (e.g. roughly 10k valid 0.5-hour observations out of a maximum possible of 17.5k). No other year shows anything close to full four-season data coverage. If the authors contend that 2014 and 2010 also provide “year-round” flux data then they have a very low standard/expectation for what constitutes valid year-round performance which they should share with readers.
I agree, the cited statement is a bit vague. I replaced
“Although data coverage is biased towards the growing season, the data set contains year-round fluxes in some years (see Table 1).”
with
Although data coverage is biased towards the growing season, the dataset contains considerably more shoulder season and winter fluxes in its second half from 2010 to 2017(see Table 1 *(in original draft)*). The also increasing availability of year-round ancillary meteorological data resulted in gap filled flux time series covering each half hour in the two years 2010 and 2016 (see Figure 1).
To illustrate data coverage better than only in Table 1 , I added a new figure containing corrected measured and gap-filled fluxes.

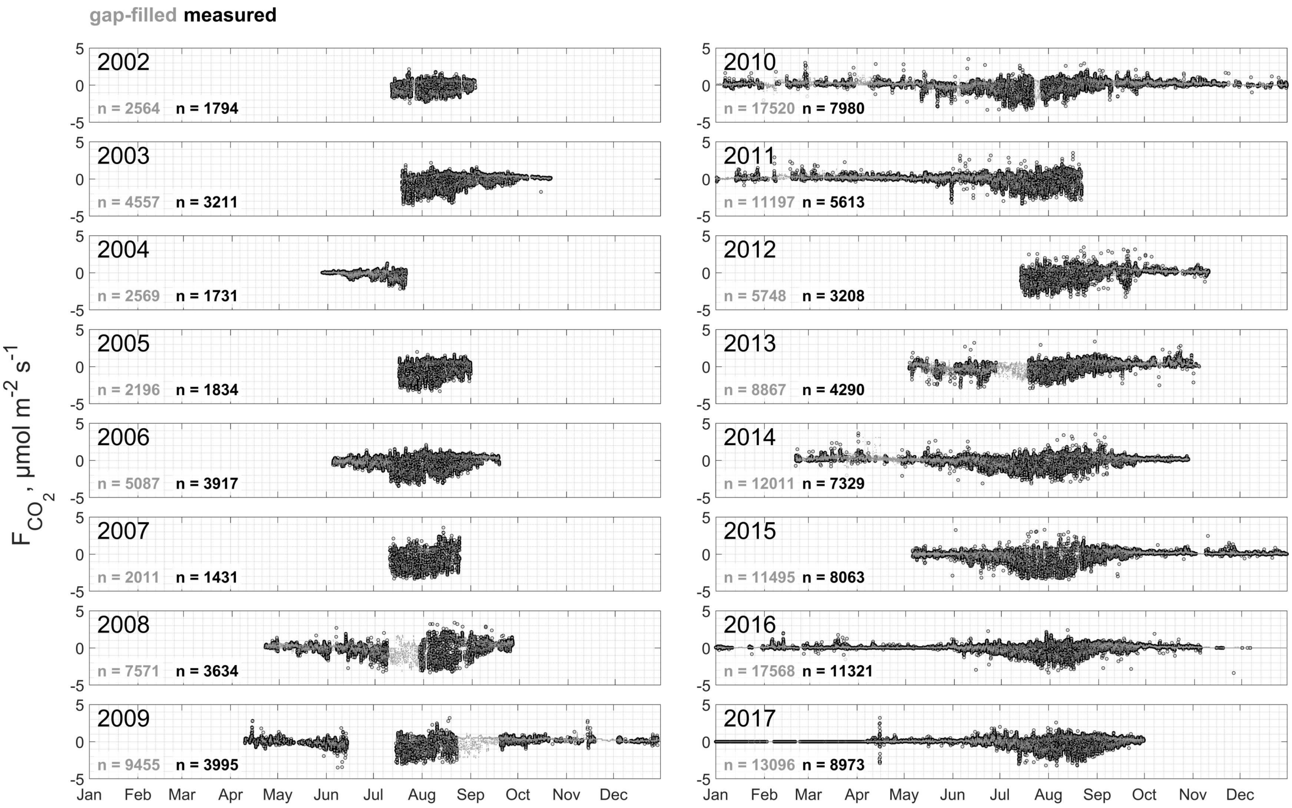

Fig. 1 Multiannual carbon dioxide flux time series compiled from fluxes measured with closed-path and open-path sensors on Samoylov Island's river terrace. Fluxes of quality class 2 are not shown. Self-heating errors in the OP dataset have been corrected for. Additionally, the result from gap filling this time series with the MDS method is shown. The given numbers of values for the gap-filled time series include measured fluxes.

RC 10

Page 6 line 4: "These Webb-Pearman-Leuning (WPL, Webb et al., 1980) terms". 'These' in this case refers to terms necessary to calculate density for OP measurements but sentence as written allows confusion. Better to specify temperature, pressure, water vapour content, etc.

RC 11

Page 6 line 7: "undisturbed heat fluxes". Reviewer may know what you mean by 'undisturbed' and why you need those, but you have not explained clearly to readers.

RC 12

Page 6 line 7: "WPL terms" By this point authors should have told readers exactly what they mean when they say 'WPL terms'. Jargon creeps in here, as well as assumption that every reader already knows the intricacies of eddy correlation measurements. Not true! Please rewrite the initial sentences of this paragraph in a clearer form and format.

Referring to comments RC 10 to RC 12: I agree, the section on the corrections for air density fluctuations are somewhat confusing and too brief. I therefore rewrote the section from page 5, line 14 (starting with "CP analyzers have the…") until page 6, line 8 (before "Major drawbacks…") and moved it to a new paragraph in an effort to include a more understandable and thorough description of the WPL approach.

Infrared gas analyzers typically measure gas densities and report the number of molecules per volume of air. To be able to refer the mass of a gas to the mass of air, gas densities are transformed to mixing ratios using air density. However, as the optical path of an OP gas analyzer is exposed to the varying temperature, pressure and humidity conditions of the atmosphere, air density in the measurement cell fluctuates mainly due to thermal expansion/contraction and water dilution/concentration. This effect, that leads to faulty concentration readings of OP instruments and thereby to incorrect flux estimates, has first been described by Webb et al. (1980). The authors proposed two flux correction terms to compensate for these density fluctuation effects that are referred to as Webb-Pearman-Leuning (WPL) terms and have since been verified experimentally and theoretically and are routinely applied in OP EC studies. Especially at times of low gas fluxes, WPL terms can become orders of magnitude larger than raw gas fluxes (Munger et al., 2012). CP analyzers have the advantage of controlled temperature and pressure conditions in the measurement cell, allowing for the sample-wise calculation of mixing ratios rather than molar densities (Ibrom et al., 2007b) and thereby avoiding the need to apply air density fluctuation correction terms after raw flux calculation.

RC 13
Why does a reader find Figs 1 and 2 introduced at appropriate points within the text but all Tables and Figs 3 and 4 appearing at the end of the manuscript after text and references. Need to fix this now and check it again during proofreading.
Figures 3 and 4 (numbering of discussion paper) were removed. See my reply to RC 15 below.
The table placement after the references is part of the ESSD guidelines for manuscript preparation.
On the website (https://www.earth-system-science-data.net/for_authors/manuscript_preparation.html) it says: "Any tables should appear on separate sheets after the references and should be numbered sequentially with Arabic numerals."
I suspect that typesetting of the final version by the publisher will result in a placement of tables closer to the references to it in the text.

RC 14
The authors' descriptions of data processing, quality filtering, self-heating corrections, temporal gap filling etc. seem appropriate and well-described. However, we find no assessment of the the two-year period of tower relocation. Mentioned in the introduction and again in the conclusions, but completely absent from the data processing and data quality descriptions. If that relocation does not matter, e.g. had no effect on time series or data quality, then readers must question the footprint analysis, as mentioned in the Conclusion! Based on lack of information here, this statement from the conclusion " … ensuring that EC source area deviations are quantifiable by a potential user" seems unsupportable for at least two years? One also wonders about the earlier documentation that sampling frequencies changed (e.g. 20 Hz to 10 Hz to briefly 5 Hz). Did those changes also have no effect (or no utility) on data processing. The authors seem to expect users to ignore these possibly substantial location sampling issues but, having mentioned both changes (good) they then fail to report corrections or consequences (bad).
I added a new "Discussion" section to the manuscript addressing these issues.
Although we did our best to ensure the consistency and appropriateness of the data processing workflow for the presented NEE time series, due to technical and logistical constraints during 16 years of field work, disparities in the experimental setup exist which may challenge its integrity. The EC tower was relocated twice, the measurement height was changed three times (see Figure 1 and Table 1 *(in original draft)*). These changes of tower location and measurement height affected the source area and hence the surface types sampled during flux measurements. Most notably, between July 2007 and June 2009, the EC tower was placed about 650 m south-west of its original position at the center of Samoylov Island, in an area with an increased coverage of the surface class *wet tundra*. This is revealed by the footprint analysis (Figure 2). While the EC footprint is dominated by the surface class *dry tundra* throughout the time series, during subperiods 2007, 2008 and 2009 I the contributions of *wet tundra* to the measured flux are significantly higher.
To check the effect of the shifts in tower location and measurement height on cumulative CO_2-C fluxes, we calculated flux sums for a period when flux time series without gaps were available in most years. The overlapping period covers days of year 200 to 234, i.e. part of the growing season in all years except for 2004 (see Figure 3). Interannual variability of cumulative C fluxes in years with constant tower location (and measurement height) appears to be large and driven by a more complex set of variables than shifts in surface class contributions only. Flux sums from the periods when EC tower relocation led to a significant shift in EC footprint composition are well within the range of the distribution of cumulated fluxes from years with a more homogeneous EC fetch area. We therefore assume that, at least with respect to budget calculations, the presented long-term time series is not disrupted and can be regarded as representative for a polygonal tundra site dominated by dry tundra. For a more in depth analysis of flux dynamics, footprint information should and can be considered by users of the data set. Recently, a comparison between surface class level NEE models based on chamber measurements with EC fluxes, using the half-hourly footprint information provided in this data set for scaling, yielded good agreement between the results obtained with both methods Eckhardt et al. (2018). We regard the availability of half-hourly footprint information in the presented NEE data set an attribute that sets it apart from other studies and holds chances for comprehensive analyses.
Apart from the changes in anemometer height, other deviations of the general instrument setup occurred due to limitations in data storage during two winter periods when the acquisition frequency was reduced to 5 Hz

and 10 Hz respectively. Rinne et al. (2008) demonstrated in a field experiment that fluxes calculated from raw data recorded at frequencies below 20 Hz compare well with fluxes derived from high frequency raw data. Differences arise as an increase of random noise and not as a systematic bias. High frequency noise removal before ensemble spectra estimation in EddyPro is effective in limiting the effect of increased noise on the quality of transfer function estimation in the process of spectral correction. Overall spectral correction in EddyPro is expressed as a spectral correction factor (SCF) which comprises the effect of all applied compensations for high and low frequency loss. Raw fluxes are multiplied with the respective SCFs during processing. We compared the SCF distributions of the two above mentioned winter periods with statistics of the remaining parts of the time series when data was recorded at 20 Hz. SCF deviations between the different acquisition frequencies are minor (see Figure 4) implying that systematic differences between fluxes calculated form raw data of different temporal resolutions are in fact small, random uncertainties increase, however.

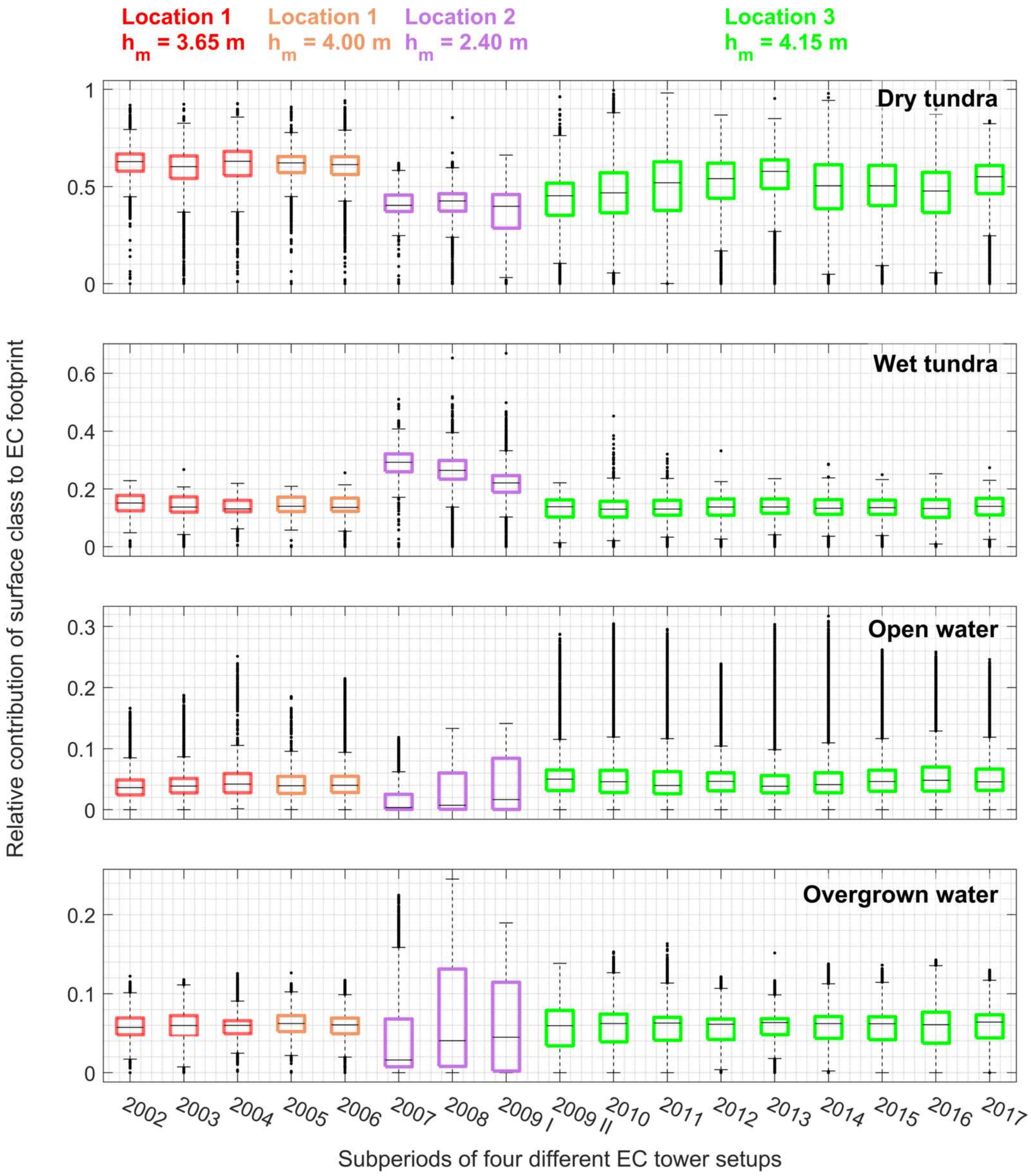

Fig. 2 Mean surface class composition of the eddy covariance footprint during 17 subperiods of four different tower setups at three locations on Samoylov Island.

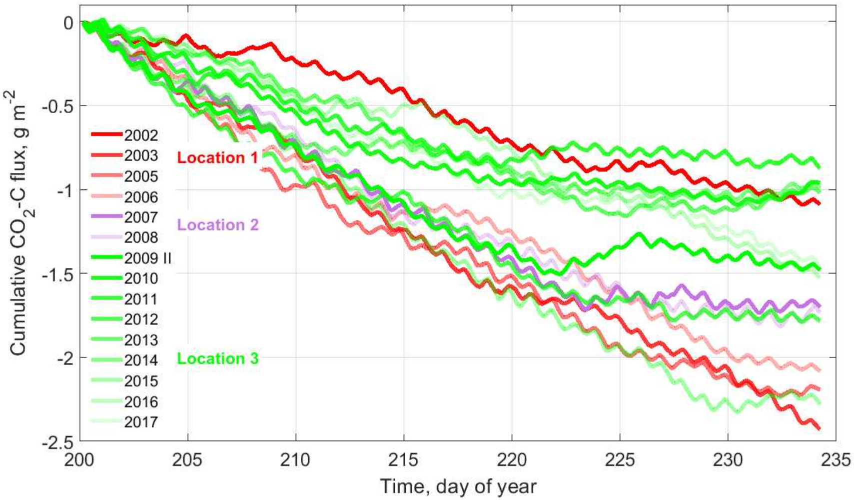

Fig. 3 Comparison of cumulative CO2 flux sums of different years during the same day of year range.

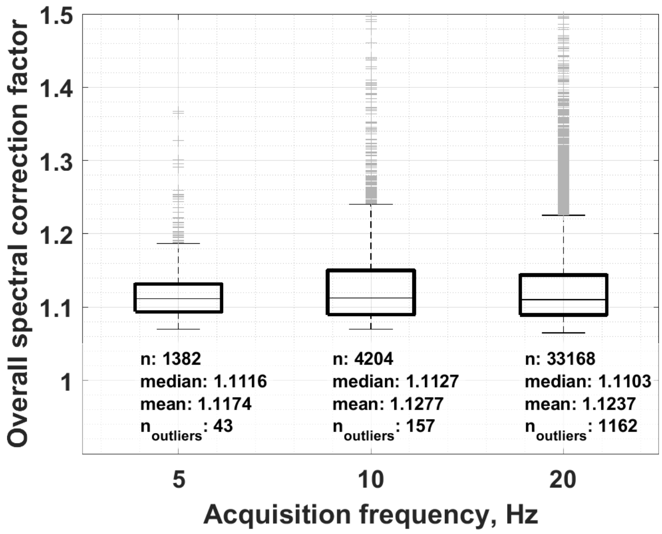

Fig. 4 Spectral correction factor statistics for periods with different acquisition frequencies.

RC 15

Fig. 4 not referenced in text? In the (barely viewable) version provided for review, Figure 3 and Figure 4 look identical, even to having identical numbers (n) of samples. The legends for the two figures differ slightly, but the figures themselves differ not at all. Wrong figure in the wrong place? Or, because we find no mention of Figure 4 in the text, one figure wrongly duplicated? Serious error, needs attention.

There is indeed a difference between Figures 3 and 4 (note that these figure numbers refer to the original draft, not the figures we see above, on this page). It is, however, fairly subtle. The difference between the plots only refers to OP fluxes, Figure 3 shows fluxes that are corrected for the self-heating effect, Figure 4 shows uncorrected fluxes, hence the number of samples are identical. My intent was for a reader to be able to flip back and forth between pages 19 and 20 in the pdf file viewed in full-screen on a computer to get a visual impression of the impact of the self-heating correction on OP fluxes. This intention clearly did not pan out, I will therefore remove Figures 3 and 4 and replace them with a new Figure (Figure 1 in this document) showing corrected measurement data and gap filled fluxes for a better overview of the final time series.

RC 16
Analysis and use of this particular CO2 data will require simultaneous access to observation time series from boreholes, river gauges, water sampling, long-term meteorology, e.g. Boike et al. 2018. Very important to connect these two data sets. If Boike et al. emerges successfully from ESSD, then we need a close explicit link described here. Until Boike et al. appear in ESSD or elsewhere, release of this data seems premature at best. If other sources of necessary soil, radiation, micrometeorlogical, etc. data exist, please reference those as well or instead? Tiksi?
I agree, the fact that long-term meteorological and soil records are available makes our NEE time series much more valuable. Boike et al. (2018) archived their data in two long-term repositories (Pangaea and Zenodo). Links are added in the following paragraph that I added to the end of the conclusion.
Furthermore, analysis of this NEE time series is not limited to the gas flux data only. An extensive data stream of meteorological and soil variables between 2002 and 2017 has recently been published by Boike et al. (2018). The authors made their records publicly accessible on the two long-term repositories Pangaea (https://doi.pangaea.de/10.1594/PANGAEA.891142) and Zenodo (https://zenodo.org/record/2223709). The fact of simultaneously available ancillary ecosystem variables enables a potential user to put the gas flux dynamics reported in this publication into context with the variability of other ecosystem properties and potential flux drivers. We regard this type of analysis as vital to understand inter-annual variability of CO_2 fluxes on Samoylov Island and are working on it ourselves (Kutzbach, unpublished).

RC 17
Note reference to methane measurements. Do these authors consider that they have now have sufficient information, biogeochemical and ecological, to construct an annual carbon budget? If so, they should at least assure readers of forthcoming analyses. If not, why not? Lack of winterseason measurements? Can only construct a valid annual budget for, e.g., 2016?
We regard this dataset publication as a starting point for analysis of flux dynamics done by us and other members of the scientific community. Yes, we think the literature record of information necessary to conduct carbon budget calculations for Samoylov Island has certainly grown over the last years. Especially the manuscript at hand contributes an important part of the information necessary to tackle the task of budget calculations successfully. As mentioned before, we are aiming at publishing those types of results in the future (Kutzbach, unpublished). In this paper, however, we wanted to focus on the methods we used to process the data rather than its interpretation. To our understanding, this proceeding is in line with the "Aims and scope" of ESSD, which is one reason why we selected this journal.
"Articles in the data section may pertain to the planning, instrumentation, and execution of experiments or collection of data. Any interpretation of data is outside the scope of regular articles. Articles on methods describe nontrivial statistical and other methods employed (e.g. to filter, normalize, or convert raw data to primary published data) as well as nontrivial instrumentation or operational methods. Any comparison to other methods is beyond the scope of regular articles." (https://www.earth-system-science-data.net/about/aims_and_scope.html)

RC 18
What makes this time series interesting? Why not simply download from FLUXNET2015? Presumably this data serves as important piece of the tundra carbon analysis presented by Zono et al.? For this reader, the authors have not made an adequate case about potential importance and utility. Readers might consider it potentially very important but this statement, again from the conclusion - "a valuable addition to the already existing data base of CO2 net ecosystem exchange observations from the Arctic" - seems weak and vague. Do the authors claim to have produced a unique high-quality data set or just another contribution to FLUXNET. If the former, then ESSD seems an appropriate venue. If the latter, why bother? Publish the entire FLUXNET data set instead? Again, this reader favours the former but the authors have not made a strong case.
We are currently talking with FLUXNET staff about how to submit our updatad time series. Some of the information we provide is beyond what one could find in a typical FLUXNET release. At this time, I am not sure if our parallel data stream of open and closed-path sensors from a single site conforms to the FLUXNET data format. For the same reason, the EC footprint data will most likely stay exclusive to the Pangaea release of this data set. While shifts in EC footprint composition are important to understand flux dynamics they are not routinely included in FLUXNET data sets. Besides the latter fact that emphasizes the uniqueness of the presented data set, I think a publication in ESSD is further justified by the revised analysis of the overall time

series consistency with respect to instrumentation and location changes as well as by the thorough description of data processing/quality filtering. Furthermore, a detailed description of site characteristics including the relevant literature put the data set into context beyond of what is possible within a FLUXNET release.

New References

Chadburn, S. E., Krinner, G., Porada, P., Bartsch, A., Beer, C., Belelli Marchesini, L., Boike, J., Ekici, A., Elberling, B., Friborg, T., Hugelius, G., Johansson, M., Kuhry, P., Kutzbach, L., Langer, M., Lund, M., Parmentier, F.-J. W., Peng, S., Van Huissteden, K., Wang, T., Westermann, S., Zhu, D., and Burke, E. J.: Carbon stocks and fluxes in the high latitudes: using site-level data to evaluate Earth system models, Biogeosciences, 14, 5143–5169, 2017.

Eckhardt, T., Knoblauch, C., Kutzbach, L., Simpson, G., Abakumov, E., and Pfeiffer, E.-M.: Partitioning CO2 net ecosystem exchange fluxes on the microsite scale in the Lena River Delta, Siberia, Biogeosciences Discussions, 2018, 1–27, 2018.

Porada, P., Weber, B., Elbert, W., Pöschl, U., and Kleidon, A.: Estimating global carbon uptake by lichens and bryophytes with a processbased model, Biogeosciences, 10, 6989–7033, 2013.

Raddatz, T., Reick, C., Knorr, W., Kattge, J., Roeckner, E., Schnur, R., Schnitzler, K.-G., Wetzel, P., and Jungclaus, J.: Will the tropical land biosphere dominate the climate–carbon cycle feedback during the twenty-first century?, Climate Dynamics, 29, 565–574, 2007.

Richardson, A. D., Aubinet, M., Barr, A. G., Hollinger, D. Y., Ibrom, A., Lasslop, G., and Reichstein, M.: Uncertainty quantification, in: Eddy Covariance: A Practical Guide to Measurement and Data Analysis, edited by Aubinet, M., Vesala, T., and Papale, D., pp. 173–209, Springer, 2012.

Richardson, A. D., Hollinger, D. Y., Burba, G. G., Davis, K. J., Flanagan, L. B., Katul, G. G., Munger, J. W., Ricciuto, D. M., Stoy, P. C., Suyker, A. E., et al.: A multi-site analysis of random error in tower-based measurements of carbon and energy fluxes, Agricultural and Forest Meteorology, 136, 1–18, 2006.

Rinne, J., Douffet, T., Prigent, Y., and Durand, P.: Field comparison of disjunct and conventional eddy covariance techniques for trace gas flux measurements, Environmental pollution, 152, 630–635, 2008.

Dragoni, D., Schmid, H. P., Grimmond, C. S. B., and Loescher, H. W.: Uncertainty of annual net ecosystem productivity estimated using eddy covariance flux measurements, Journal of Geophysical Research: Atmospheres, 112, 2007.

A long-term (2002 to 2017) record of closed-path and open-path eddy covariance CO_2 net ecosystem exchange fluxes from the Siberian Arctic

David Holl[1], Christian Wille[2], Torsten Sachs[2], Peter Schreiber[3], Benjamin R.K. Runkle[4], Lutz Beckebanze[1], Moritz Langer[3], Julia Boike[3,8], Eva-Maria Pfeiffer[1], Irina Fedorova[5], Dimitry Yu. Bolshianov[6], Mikhail N. Grigoriev[7], and Lars Kutzbach[1]

[1]Institute of Soil Science, Center for Earth System Research and Sustainability (CEN), Universität Hamburg, Hamburg, Germany
[2]Helmholtz-Zentrum Potsdam – Deutsches GeoForschungsZentrum (GFZ), Potsdam, Germany
[3]Alfred Wegener Institute Helmholtz Centre for Polar and Marine Research, Potsdam, Germany
[4]Department of Biological & Agricultural Engineering, University of Arkansas, Fayetteville, USA
[5]Saint Petersburg State University – Institute of Earth Sciences, St. Petersturg, Russia
[6]Arctic and Antarctic Research Institute, St. Petersburg, Russia
[7]Permafrost Institute, Yakutsk, Russia
[8]Humboldt-Universität zu Berlin, Geography Department, Berlin, Germany

Correspondence: David Holl (david.holl@uni-hamburg.de)

Abstract. Ground-based observations of land–atmosphere fluxes are necessary to progressively improve global climate models. Observed data can be used for model evaluation and to develop or tune process models. In arctic permafrost regions, climate–carbon feedbacks are amplified. Therefore, increased efforts to better represent these regions in global climate models have been made in recent years. We present a multiannual time series of land–atmosphere carbon dioxide fluxes measured *in situ* with the eddy covariance technique in the Siberian Arctic (72° 22' N, 126° 30' E). The site is part of the international network of ~~carbon dioxide~~ eddy covariance flux observation stations (FLUXNET, Site ID: Ru-Sam). The ~~dataset~~ data set includes consistently processed fluxes based on concentration measurements of closed-path and open-path gas analyzers. With parallel records from both sensor types, we were able to apply a site-specific correction to open-path fluxes. This correction is necessary due to a deterioration of data, caused by heat generated by the electronics of open-path gas analyzers. Parameterizing this correction for subperiods of distinct sensor setups yielded good agreement between open and closed-path fluxes. We compiled a long-term (2002 to 2017) carbon dioxide flux time series that we additionally gap-filled with a standardized approach. The data set was uploaded to the Pangaea data base and can be accessed through https://doi.pangaea.de/10.1594/PANGAEA.892751.

1 Introduction

The release of the Arctic's belowground carbon (C) pools to the atmosphere can potentially act as a positive feedback on climate change. Organic material that is now stored in the permanently frozen soil and largely inaccessible for microbial decomposition might become available under a warming climate resulting in an increased release of greenhouse gases from Arctic regions (Schuur et al., 2015). At the same time, the Arctic vegetation responds to ongoing warming with a greening trend (Park et al., 2016), probably enhancing summer carbon assimilation. Although the importance of permafrost carbon pools for a potential amplification of climate change has been widely recognized (e.g. Zimov et al., 2006; Davidson and Janssens, 2006; Schuur et al., 2008; Khvorostyanov et al., 2008; Tarnocai et al., 2009; Koven et al., 2011; Schneider von Deimling et al., 2012; MacDougall et al., 2012; Schuur et al., 2013; McGuire et al., 2018), the earth system models analyzed for the Fifth Assessment Report (AR5) of the Intergovernmental Panel on Climate Change (IPCC) did not include permafrost carbon emissions.

While efforts to include permafrost dynamics into global climate models have been made recently (e. g. Wania et al., 2009a, b, 2010; Ekici et al., 2014; Kaiser et al., 2017; McGuire et al., 2018), models can be improved by using ground-based flux measurements for calibration and validation. McGuire et al. (2012) assessed the carbon balance of the Arctic tundra combining ground-based observations, process and atmospheric inversion models. The authors found that the uncertainty with which a carbon balance can be quantified is still very large, with upper and lower uncertainty bounds indicating the Arctic tundra as a sink for carbon at one and as a C-source at the other bound. McGuire et al. (2012) conclude that ~~constraining inversion models~~ reducing uncertainties of regional estimates based on observational data relies on high quality ground-based measurements that should be placed strategically, e. g. along hydrological or vegetation gradients. *In situ* gas flux measurements from the Arctic are, however, still scarce. Moreover, the available data is biased towards Alaska, observations from the Eurasian Arctic are even more scarce (Oechel et al., 2014). To be able to distinguish climate change-related flux responses from interannual variability, long-term ~~datasets~~ data sets are essential as recently argued by Baldocchi et al. (2017).

Within the scope of this publication, we aimed at creating a high quality, long-term CO_2 flux ~~dataset~~ data set from a polygonal tundra site in the Russian Arctic. We had the opportunity to analyze a 16 year record of eddy covariance data that includes periods with simultaneous measurements from two different (closed-path and open-path) CO_2 gas analyzer types. Our objective was to consistently process the data while following standardized quality control methods to allow for comparability between the different years of our record and with other ~~datasets~~data sets. We additionally aimed at cross-calibrating open-path and closed-path CO_2 fluxes and at gap-filling the ~~dataset~~ data set by employing the method of Reichstein et al. (2005) that is widely used in the FLUXNET community.

2 Site description

The investigation site is located on Samoylov Island in the southern central part of the Lena River Delta at 72° 22' N, 126° 30' E (see Figure 1). The fan-shaped delta covers an area of roughly 30000 km^2 (Grigoriev, 1993; Schneider et al., 2009) and is characterized by a network of channels and more than 1500 islands (Antonov, 1967). Being the largest delta in the Arctic and one of the largest worldwide (Walker, 1998), it lies in the continuous permafrost zone with permafrost depths of about 500

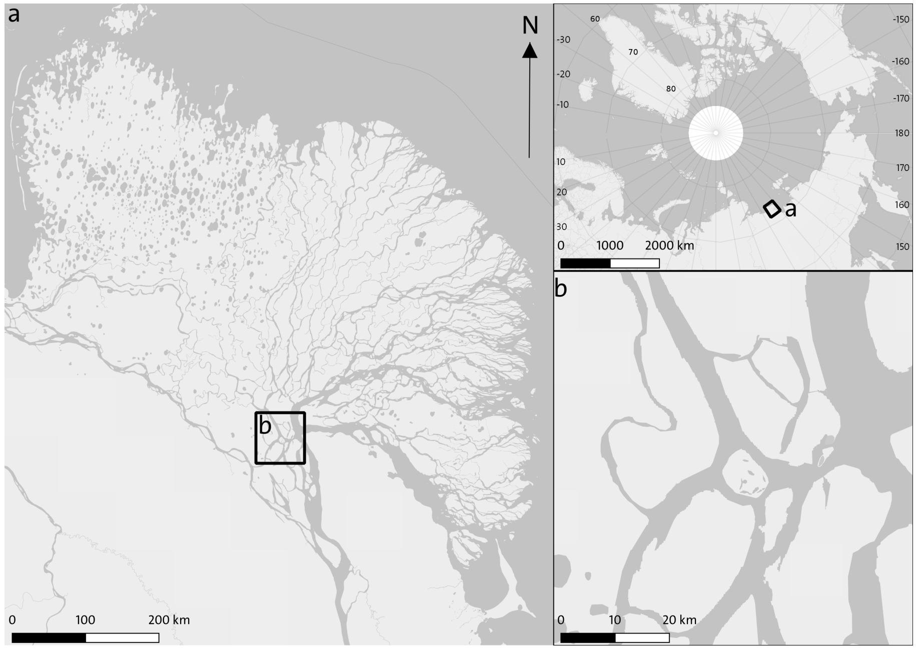

Figure 1. Location of Samoylov Island (center of panel b) in the Lena River Delta (panel a). Map data from: OpenStreetMap contributors, under Open Database License

to 600 m (Romanovskii et al., 2004; Yershov, 2004; Brown et al., 1997). Mean annual permafrost temperatures range around -9 °C at 10 m depth (Romanovsky et al., 2010), making the Lena River Delta one of the coldest permafrost regions on earth. Boike et al. (2013) inferred an annual mean soil temperature of -8.6°C at 10.7 m depth from a 2006 to 2011 time series of temperature measurements in a borehole on Samoylov Island. Based on long-term hydrological observations in the delta area, Fedorova et al. (2015) found an increase in discharge as well as in sediment flux indicating recently intensified thawing of ice complex sediments in the region.

Grigoriev (1993) divides the delta area in three main geomorphological units. The oldest, ice-rich river terrace consists of fine-grained sediments with high organic content. It developed as an eroded Pleistocene plane characterized by polygonal ground and thermokarst processes. The second largest unit consists of Late Pleistocene to Early Holocene sandy sediments with low ice content and covers 23 % of the north-western part (Schneider et al., 2009). Samoylov Island is part of the third unit, the Mid to Late Holocene river terrace (Bolshiyanov et al., 2015), which makes up about two thirds of the delta (Schwamborn et al., 2002).

The island itself consists of two morphological units, an annually flooded, modern floodplain (1.49 km^2) in the west and a Late Holecene river terrace (2.85 km^2) in the east, which lies 10 to 16 m a.s.l. and is not flooded regularly (Kutzbach et al., 2007; Boike et al., 2013). The data presented here was collected with ~~an eddy covariance system~~ eddy covariance systems installed on the elevated river terrace. In contrast to the modern floodplain, the river terrace's surface is patterned due to frost-action that formed a wet polygonal tundra landscape consisting of mostly low-centered and some high-centered ice-wedge polygons as well as thermokarst lakes and channels. Due to the underlying permafrost and thereby hampered drainage, water-saturated soils or ponds form in the polygon centers, whereas on the rims, which can be elevated up to 50 cm above the centers, a drier, moderately moist water regime prevails (Kutzbach et al., 2007; Helbig et al., 2013). Accordingly, the vegetation community in the wetter centers is dominated by hydrophytic sedges (*Carex aquatilis*, *Carex chordorrhiza*, *Carex rariflora*) and mosses (e. g. *Limprichtia revolvens, Meesia longiseta, Aulacomnium turgidum*). Mesophytic dwarf shrubs (e. g. *Dryas octopetala, Salix glauca*), forbs (e. g. *Astragalus frigidus*) and mosses (e.g. *Hylocomium splendens, Timmia austriaca*) dominate on the rims (Kutzbach et al., 2004; Pfeiffer and Grigoriev, 2002). Maximium summer leaf coverage was estimated by Kutzbach et al. (2004) to be 0.3 for vascular plants and 0.95 for mosses and lichens at both polygon centers and rims. The river terrace as a whole is composed of polygon rims with a coverage of 60 to 65 % and of depressed surfaces (including vegetated and water filled polygon centers as well as lakes and channels) that cover the remaining 35 to 40 % of area (Kutzbach et al., 2007; Sachs et al., 2010; Muster et al., 2012; Boike et al., 2013).

An arctic-continental climate with low mean annual temperatures prevails in the Lena River Delta. Although precipitation is low as well, the climate can be considered humid as evaporation rates are low due to low ~~evaporation rates~~ ambient temperatures and relative humidity is high (Kutzbach, 2006; Boike et al., 2008; Langer et al., 2011a, b). Based on long-term (1998 to 2017) *in situ* measurements on Samoylov Island, Boike et al. (2018) inferred an annual mean air temperature of -12.3 °C; the coldest and warmest months being February and July with mean temperatures of -32.7 °C and 9.5 °C respectively. For the period from 1998 to 2011, Boike et al. (2013) estimated total annual precipitation to be composed of 124 $\pm$ 57 mm summer rainfall and 65 $\pm$ 35 mm snowfall. Interannual variability in rainfall was, however, very high, with a maximum of 199 mm and a minimum of 48 mm. Snow melt usually starts in mid-May and lasts until early June. Snow accumulation typically commences between late September and early October. Between 1998 and 2011, the snow season lasted on average 224 $\pm$ 18 days, the snow-free ~~periond~~ period 138 $\pm$ 18 days. Snow depth was reported by Boike et al. (2018) averaging 0.3 m between 2002 and 2017 with a maximum of 0.8 m in 2017. Beginning in early to mid-June, the soil starts to thaw from the top, forming the so called active layer. Boike et al. (2013) report a mean active layer depth in August of 49 cm with a maximum of 79 cm between 1998 and 2011. The closest WMO (World Meteorological Organisation) weather station is located on the continent, around 110 km southeast from Samoylov Island in the city of Tiksi (WMO ID 21824). Between 1936 and 2017 the mean air temperature reported from Tiksi is - 12.74 °C, mean annual precipitation amounts to 304.5 mm (AARI, 2018). While the mean air temperature in Tiksi is very similar to the 20-year mean from Samoylov Island, average annual precipitation appears to be much higher in Tiksi than in the delta region. Boike et al. (2013) explain this divergence with the fact that Tiksi is located at the coast of the Laptev sea and surrounded by mountains.

The soils of Samoylov Island were classified as *Gelisols* by Zubrzycki et al. (2013) based on work by Pfeiffer and Grigoriev (2002) according to the US Soil Taxonomy (Soil Survey Staff, 2014). On subgroup level, typical soils of the river terrace are *Glacic Aquiturbels*, which developed on the polygon rims and are characterized by the translocation of soil material due to freeze-thaw processes (cryoturbation). In the wetter polygon centers *Typic Historthels* formed. On the more sand-rich active floodplain, *Typic Aquorthels* and *Typic Psammorthels* dominate. According to the FAO World Reference Base for Soil

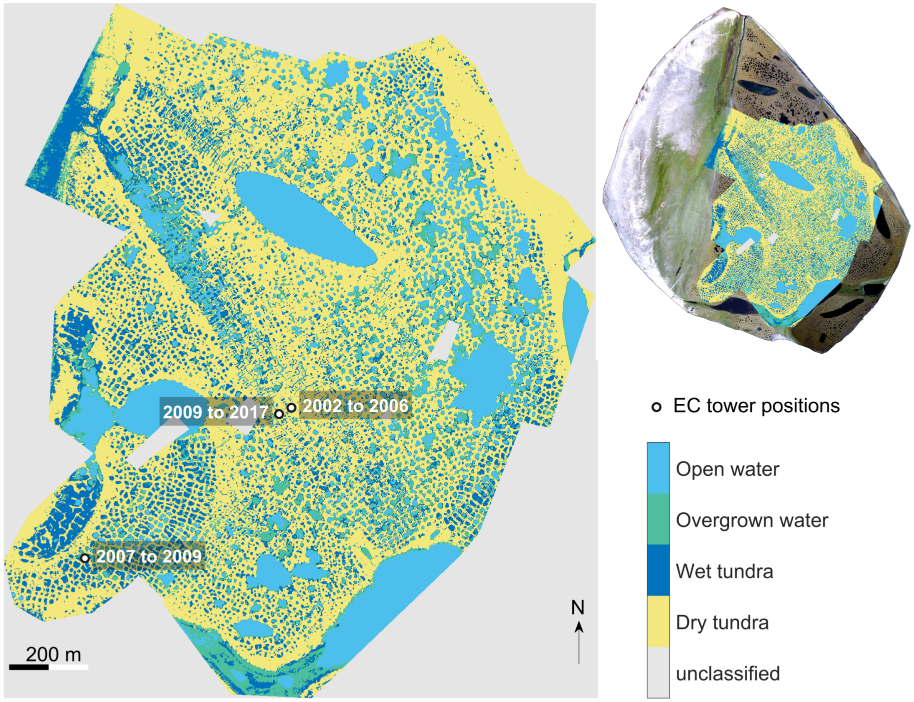

Figure 2. Eddy covariance (EC) tower positions on the river terrace of Samoylov Island and surface class distribution according to Muster et al. (2012). Photographic image of the entire island (top right corner) from Boike et al. (2012).

Ressources (IUSS Working Group WRB, 2015), the diverse soils of Samoylov Island belong to the reference soil group of *Cryosols*. Zubrzycki et al. (2013) estimated the soil organic carbon (SOC) stocks for the upper meter of the island's two major landscape units to be $29 \pm 10\,\mathrm{kg\,m^{-2}}$ for the river terrace and $14 \pm 7\,\mathrm{kg\,m^{-2}}$ for the active floodplain.

~~Since the scientific investigation of Samoylov Island commenced, gas exchange between the soils of the island and the atmosphere has been a research focus. While results on methane exchange fluxes and the soils' methane production and oxidation potential are more prominent in the publication record (e.g. Wagner et al., 2003; Kutzbach et al., 2004; Liebner and Wagner, 200, literature on CO_2 flux time series recorded with the same measurement system presented in this publication is available as well (Kutzbach, 2006; Kutzbach et al., 2007; Runkle et al., 2013; Zona et al., in review). The micrometeorological station on Samoylov Island is part of the international network of EC carbon dioxide flux observation sites (FLUXNET, Site ID: Ru-Sam). Kutzbach et al. (2015) contributied EC flux data from this measurement system to the FLUXNET2015 dataset.~~

3 Methods

3.1 Instrumentation

We used the eddy covariance (EC) technique to determine half-hourly gas and energy fluxes. The EC method requires high frequency (typically > 10 Hz) raw gas concentration and three-dimensional wind speed velocity measurements. A comprehensive description of the EC approach is given for example by Aubinet et al. (2012). We recorded carbon dioxide (CO_2) and water vapor concentrations as well as three-dimensional wind speed velocity with changing instrumentation on three different tower structures, all located on the central river terrace of Samoylov Island between 2002 and 2017 (see Fig. Figure 2). We deployed open-path (OP) as well as closed-path (CP) gas analyzers, at times simultaneously. Models, manufacturers and years of deployment are given in Table 1. Between the different setups, CP intake tube lengths varied from 5 to 8 m. OP analyzers were always installed inclined by about 10 degrees from the vertical, as suggested in the analyzer manuals. Raw data was recorded at 20 Hz except for the periods 22 August 2009 to 19 July 2010 (10 Hz) and 31 August 2012 to 17 May 2013 (5 Hz). Until 29 April 2014, all raw data were recorded on a CR3000 data logger (Campbell Scientific, UK). From then on, CP analyzer and anemometer data were logged on a CR3000 whereas OP analyzer and anemometer data were recorded on a LI-7550 data logger (Licor Biosciences, USA). Although data coverage is biased towards the growing season, the data set contains year-round fluxes in some years considerably more shoulder season and winter fluxes in its second half from 2010 to 2017(see Table 1). The also increasing availability of year-round ancillary meteorological data resulted in gap-filled flux time series covering each half hour of the two years 2010 and 2016 (see Figure 4).

3.2 Flux processing

3.2.1 Prior considerations

Due to the contrasting designs of OP and CP analyzers, these sensor types have distinct signal response characteristics that we considered during data processing. The most apparent constructional difference between OP and CP gas analyzers is the presence or absence of a housing for the measurement cell that contains the optical path. In a CP instrument, the measurement cell is housed whereas the optical path of an OP analyzer is exposed to the atmosphere. CP systems are typically more bulky and installed at the base of an EC tower, from where tubing leads to an intake close to the anemometer. Sample air is drawn into the cell with a pump. OP sensors are commonly installed in close proximity to the anemometer and do not require a pump that greatly reduces the power consumption of OP instruments compared to CP setups. Due to the tubing acting as a low-pass filter, the response to high-frequency concentration variations is systematically attenuated in CP setups, as opposed to OP systems (Ibrom et al., 2007a). Moreover, the severity of frequency dampening can vary non-linearly with environmental conditions, especially with relative humidity (Runkle et al., 2012). CP analyzers have the advantage of controlled temperature and pressure conditions in the measurement cell, allowing for the calculation of mixing ratios rather than molar densities (Ibrom et al., 2007b) and thereby avoiding the need to apply air densityfluctuation correction terms.

~~These Webb-Pearman-Leuning (WPL, Webb et al., 1980) terms have to be included when using OP data to calculate EC fluxes~~Infrared gas analyzers typically measure gas densities and report the number of molecules per volume of air. To be able to refer the mass of a gas to the mass of air, gas densities are transformed to mixing ratios using air density. However, as the optical path of an OP gas analyzer is exposed to the varying temperature, pressure and humidity conditions of the atmosphere~~. Additional sources of uncertainty are introduced when applying WPLterms, as their quality relies on not only precise but accurate concentration measurements as well as on undisturbed heat fluxes.~~ , air density in the measurement cell fluctuates mainly due to thermal expansion/contraction and water dilution/concentration. This effect, that leads to faulty concentration readings of OP instruments and thereby to incorrect flux estimates, has first been described by Webb et al. (1980) . The authors proposed two flux correction terms to compensate for these density fluctuation effects that are referred to as Webb-Pearman-Leuning (WPL) terms and have since been verified experimentally and theoretically and are routinely applied in OP EC studies. Especially at times of low gas fluxes, WPL terms can become orders of magnitude larger than raw gas fluxes (Munger et al., 2012). CP analyzers have the advantage of controlled temperature and pressure conditions in the measurement cell, allowing for the sample-wise calculation of mixing ratios rather than molar densities (Ibrom et al., 2007b) and thereby avoiding the need to apply air density fluctuation correction terms after raw flux calculation.

Major drawbacks of OP instruments, especially in harsh environments, are (1) their downtime during adverse weather conditions (e. g. precipitation) and (2) flux biases due to sensor self-heating (Burba et al., 2006, 2008). The OP self-heating effect was first recognized (Burba et al., 2006) due to apparent off-season CO_2 uptake in flux time series obtained with LI-7500 (LI-COR Biosciences, USA) OP gas analyzers. However, Kittler et al. (2017) recently found that this effect is not limited to cold conditions but extends throughout all seasons. The necessary corrections can be substantial but decrease largely when the sensor is not mounted vertically but inclined instead as shown by Rogiers et al. (2008) and Järvi et al. (2009).

3.2.2 Processing steps

We performed separate flux processing steps on OP and CP data sets and computed half-hourly fluxes using the software EddyPro (Licor Biosciences, USA). An overview of the processing steps is given in Table 2. We detected and removed raw data spikes according to Vickers and Mahrt (1997), with a maximum of 1 % accepted spikes and a maximum of three samples as consecutive outliers. We applied an angle of attack correction, i.e. compensation for flow distortion induced by the anemometer frame (Nakai et al., 2006), on wind ~~speed~~ velocity data collected with the R3 (Gill Instruments Ltd., UK) anemometer. The majority of the wind ~~speed~~ velocity records come, however, from a CSAT3 (Campbell Scientific, UK) instrument for which this correction is not necessary. Coordinate rotation to align the anemometer x-axis to the current mean streamlines was calculated as double rotation according to Kaimal and Finnigan (1994). For OP fluxes, we compensated for air density fluctuations due to thermal expansion/contraction and water dilution/concentration following Webb et al. (1980). Because simultaneous water vapor concentration, cell temperature and cell pressure measurements from inside the CP analyzer were available, CO_2 concentrations from this sensor could be converted directly into mixing ratios, i.e. concentrations referring to dry air of constant temperature (Ibrom et al., 2007b; Burba et al., 2012), making further corrections for density fluctuations unnecessary. We compensated CP time lags by using the automatic timelag optimization option in EddyPro. For this procedure, prior to processing the complete ~~dataset~~data set, time lags were determined for a subperiod of raw data by covariance maximization (Fan et al., 1990). A searching window around the median of the found time lags (nominal timelag, T_{nom}) is defined by $T_{nom} \pm 3.5 \times MAD$, where MAD is the median absolute deviation of the found time lags. When processing the complete ~~dataset~~data set, EddyPro performed a covariance maximization of vertical wind ~~speed~~ velocity and the scalar of interest for each half hour and then checked, whether the found time lag fell within the searching window defined before. If not, T_{nom} was used as time lag. Water vapor concentration time series were binned in ten RH-classes, and the procedure was applied to each class, resulting in ten different nominal time lags. CO_2 concentrations were not binned in humidity-classes. We computed CP time lag statistics annually and within a year if pump speeds or instrumental setups varied. OP time lags were determined by covariance maximization within a searching window of -10 to 10 seconds. We evaluated OP time lags statistics, binned in classes of wind direction sectors, later on in the course of quality filtering.

Spectral attenuation in the high- and the low-frequency spectral range was compensated according to the following methods. Low-frequency signal loss due to the finite averaging time used for flux calculations (30 minutes) and due to linear raw data detrending was corrected for following the method of Moncrieff et al. (2004) for both OP and CP fluxes. High-frequency signal loss of OP fluxes due to path and volume averaging of the sonic anemometer and the gas analyzers as well as due to the separation between the two instruments were corrected for with the analytical approach of Moncrieff et al. (1997). High-frequency signal loss of CP fluxes due to spectral attenuation by the intake tube and volume averaging in the measurement cell were corrected for using the *in situ* method of Ibrom et al. (2007a). For each measurement period with a unique instrumental setup and CP pump speed, we determined the cut-off frequency of a first-order low-pass filter from ensemble means of 30-minute power spectra of CO_2 concentration and sonic temperature time series data. The spectral correction factor was then parametrized as a function of the cut-off frequency found and the mean wind speed for stable and unstable atmospheric conditions as described by Ibrom et al. (2007a). Before using them for ensemble spectra estimations, the 30-minute power spectra were quality-filtered by applying the scheme of Vickers and Mahrt (1997), and by omitting half-hours that were assigned quality class 2 according to Mauder and Foken (2004). High frequency noise was removed from the ensemble means of CO_2 concentration power spectra before the determination of the cut-off frequency where it was deemed necessary. High-frequency signal losses due to crosswind and vertical separation of the sample air tube intake and the anemometer were corrected for according to Horst and Lenschow (2009). ~~Additionally, we~~

3.3 Quality filtering

We set EddyPro to calculate ~~random flux uncertainty estimates (Finkelstein and Sims, 2001) and three quality flags , which~~ quality flags according to Mauder and Foken (2004) that represent flux quality in ~~values from~~ three classes (0~~to~~ , 1 and 2) with 0 denoting the highest ~~quality class as proposed by Mauder and Foken (2004)~~and 2 denoting the lowest quality class. This quality evaluation is based on tests for stationarity and developed turbulence and thereby indicates whether general EC assumptions about atmospheric conditions were met during a flux calculation period.

3.4 Quality filtering

Flux quality assessment was largely based on the scheme of Mauder and Foken (2004), representing flux quality in three classes (0, 1 and 2). We applied additional . In the data set available for download, we included one column for each analyzer type containing this quality flag. Additionally, we applied six further screening steps and flagged fluxes of low quality. If a flagged flux was not already assigned to class 2 according to Mauder and Foken (2004)Mauder and Foken (2004), we set the quality flag to 2. We performed In our opinion, fluxes of quality class 2 should be omitted from further analysis. They are included in the reported data set for the sake of completeness. We performed the six additional flagging steps in the following sequence. An overview of these filtering steps including the number of flagged values is given in Tabele 3.

In **step 1**, skewness and kurtosis were computed with EddyPro for the half-hourly high frequency raw data time series of CO_2 concentration, vertical wind speed and sonic temperature. If any of these statistics was outside certain intervals (skewness: $[-2,2]$, kurtosis: $[1,8]$, equivalent to the hard flag defined by Vickers and Mahrt (1997)), CO_2 flux values were flagged.

In **step 2**, OP fluxes were additionally filtered for an instrument signal strength indication (AGC) recorded from the LI-7500 sensor. Along with a software upgrade, this diagnostic value was renamed to $RSSI$, and its definition was changed. We therefore recalculated the AGC values for sensors not running on firmware version 6.6 and above (before July 2013). According to the old AGC definition in the LI-7500 manual, typical clean window values range between 55 to 65 %. As dirt accumulates on the windows (or anywhere in the optical path), the AGC value will increase up to 100 %. The new $RSSI$ value takes 100 % for clean windows and decreases as windows get dirtier. In order to obtain one consistent diagnostic variable for the cleanness of the optical path, AGC was converted to the $RSSI$ range. AGC values smaller than 44 were set to 44, then AGC values were mapped to the RSSI range as follows.

$$RSSI(AGC) = 188 - 2 \cdot AGC \qquad (1)$$

We flagged OP CO_2 flux values when $RSSI \leq 60$.

As quality control of the half-hourly time lag detection results was not applied during OP flux processing in EddyPro, we additionally screened OP time lags to identify low quality flux values in **step 3**. We divided the time lag data set into subsets of different instrumental setup, and binned the time lags of these subsets in 36 ten degree wind direction sectors. We used the 25th and 75th percentiles per class as filter thresholds. We flagged OP flux values with associated time lags outside the range spanned by these thresholds. Because we computed CP fluxes in EddyPro considering and compensating for low time lag detection quality, we did not perform this type of filtering step on CP fluxes.

In **step 4**, we flagged CP as well as OP fluxes when 30 minute average concentration measurements were larger than 450 ppm or smaller than 300 ppm. CO_2 concentrations outside this range indicate dirty OP gas analyzer optics or technical problems of the CP air sampling system (sudden pump speed changes due to brownouts, blocked filters, etc.).

To filter dubious, large OP fluxes that coincided with reasonable CP fluxes, we seleced all OP fluxes when simultaneously measured CP values ranged between -2 $\mu mol\,m^{-2}\,s^{-1}$ and 2 $\mu mol\,m^{-2}\,s^{-1}$. **Step 5** only affected OP data from this subset. We calculated the 99th and 1st percentile of this group and flagged fluxes from it when they lay outside this percentile range.

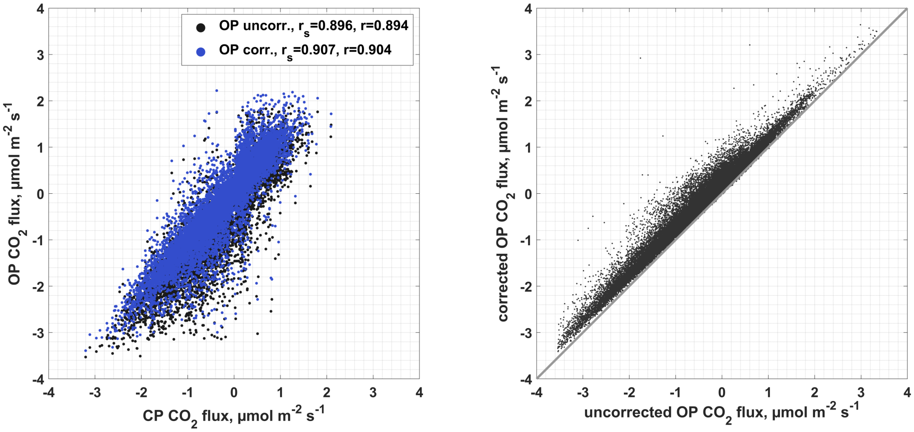

Figure 3. ~~Fluxes from~~ Effect of the self-heating correction on the correlation between open-path (OP) and closed-path (CP) ~~versus open-path~~ fluxes (~~OP~~left panel)~~analyzers~~. ~~The agreement between CP and OP fluxes increases throughout all quality classes after OP correction.~~ Correlations were quantified using Spearman~~'~~'s rank correlation coefficient r_s and Pearson~~'~~'s correlation coefficient r. ~~The right panel in~~ Only quality class 0 is shown. Negative fluxes are affected more strongly by the ~~bottom row shows the effect of the applied self-heating~~ correction ~~on OP~~ than positive fluxes (right panel).

In **step 6**, we flagged remaining outliers in both the CP and OP data sets by using the 0.1st and 99.9th percentile (-3.5423 $\mu\mathrm{mol\,m^{-2}\,s^{-1}}$ and 3.3473 $\mu\mathrm{mol\,m^{-2}\,s^{-1}}$) of the CP time series after the concentration limits filter as absolute limits, to define an acceptable range of OP and CP flux values. ~~In the dataset available for download, we included one column for each analyzer type containing a quality flag that can take values from 0 to 2 based on the scheme of Mauder and Foken (2004). As described above, we additionally assigned fluxes that did not meet our quality criteria to quality class 2. In our opinion, fluxes of quality class 2 should be omitted from further analysis. They are included in the reported dataset for the sake of completeness.~~

3.4 Open-path self-heating correction

To account for self-heating errors induced by the LI-7500 sensor electronics, we corrected OP fluxes as described by Kittler et al. (2017). The authors use WPL-corrected fluxes and add a correction term (Burba et al., 2006) that accounts for self-heating effects of vertically installed instruments. In their approach, Kittler et al. (2017) use a scaling factor ξ, taking values between 0 and 1, to trim the correction for inclined analyzer setups. With simultaneously available CP fluxes, we were able to estimate this scaling factor specifically for our site and periods of unique instrumental setups. As suggested by Kittler et al. (2017), we optimized this parameter with a nonlinear least squares method in Matlab (v. 9.2). We determined ξ for periods of different instrumental setups and separately for night (incoming shortwave radiation $< 20\ \mathrm{Wm^{-2}}$) and day (incoming shortwave radiation $\geq 20\ \mathrm{Wm^{-2}}$) conditions using the following equation

$$F_c = F_{c,WPL} + \xi \frac{(T_s - T_a)\rho_c}{r_a T_a} \quad (2)$$

where F_c ($\mathrm{kg\,m^{-2}\,s^{-1}}$) is the true CO_2 flux, $F_{c,WPL}$ ($\mathrm{kg\,m^{-2}\,s^{-1}}$) is the WPL-corrected OP CO_2 flux, T_s (K) is the instrument surface temperature, T_a (K) the ambient air temperature, r_a ($\mathrm{sm^{-1}}$) the aerodynamic resistance and ρ_c ($\mathrm{kg\,m^{-3}}$) the ambient CO_2 density. Prior to ξ optimization, we estimated the instrument surface temperature T_s following the parameterization of Järvi et al. (2009) also separately for nighttime and daytime

$$T_{s,day} = 0.93(T_a - T_0) + 3.17 + T_0 \quad and \quad T_{s,night} = 1.05(T_a - T_0) + 1.52 + T_0 \tag{3}$$

with $T_{s,day}$ (K) and $T_{s,night}$ (K) as instrument surface temperature estimates and T_0 set to 273.15 K. We determined the scaling factor as a parameter of equation (2) being the modified Burba et al. (2006) approach from Kittler et al. (2017). For function fitting, we assumed CP fluxes of quality classes 0 and 1 as true fluxes. We used WPL-corrected OP quality class 0 fluxes and the above described surface temperature estimates as independent variables. Before parameter optimization, we quality-screened the Burba et al. (2006) correction term (expression to the right hand side of ξ in equation (2)) and removed spikes ranging within the uppermost or lowest percent of its distribution. Throughout all years, ξ is larger at daytime than at nighttime but generally small, adding mostly below 1 % of the full correction term to the uncorrected flux (see Table 4). In four of the seven available years with simultaneous CP and OP fluxes, nighttime ξ optimization converged to values below zero. Before applying the correction models to these periods, we set nighttime ξ estimates to the median of the years yielding parameter values that, including their 95 % confidence bounds, ranged above zero. We used this value and the median of all daytime model optimizations to calculate corrected OP fluxes at times without parallel CP measurements. We did not correct OP fluxes when radiation measurements or correction term estimates were not available. Correlation between CP and OP fluxes improved throughout all quality classes by applying the self-heating correction (see Table 5), while fluxes indicating net CO_2 uptake were affected more strongly than fluxes above zero (see Fig. Figure 3).

3.5 Carbon dioxide flux gap filling

We used the CP and the corrected OP fluxes (see Fig. Figure 4) to compile a CO_2 flux time series. We aimed at keeping as many measured data points as possible, while omitting records with large uncertainty. We accepted all CP values of quality classes 0 and 1. At time steps where no CP fluxes were available, we selected OP values of the same quality classes. The resulting time series contains 75,921 datapoints. Additionally, we filled the remaining gaps in the time series using the marginal distribution sampling (MDS) method as first presented by Reichstein et al. (2005). This method employs two types of model value calculations. The environmental variables global radiation, air temperature and water vapour pressure deficit are binned in classes and combined in a look-up table (LUT). In case of a gap, flux values related to similar environmental conditions can be looked up and used for averaging and gap filling. The setup of different LUTs for fixed time periods has been first described by Falge et al. (2001). This process can be refined by the use of moving time windows (Moffat et al., 2007) around gaps, as applied by Reichstein et al. (2005). The second model type implemented in the MDS algorithm exploits the commonly high autocorrelation of gas flux time series. The mean diurnal variation (MDV) technique has as well been first described by Falge et al. (2001) and uses the average of available gas flux measurements from adjacent days at the same hour of day to fill a flux gap. The MDS method found wide application, as it has for example been the standard technique within the processing pipeline

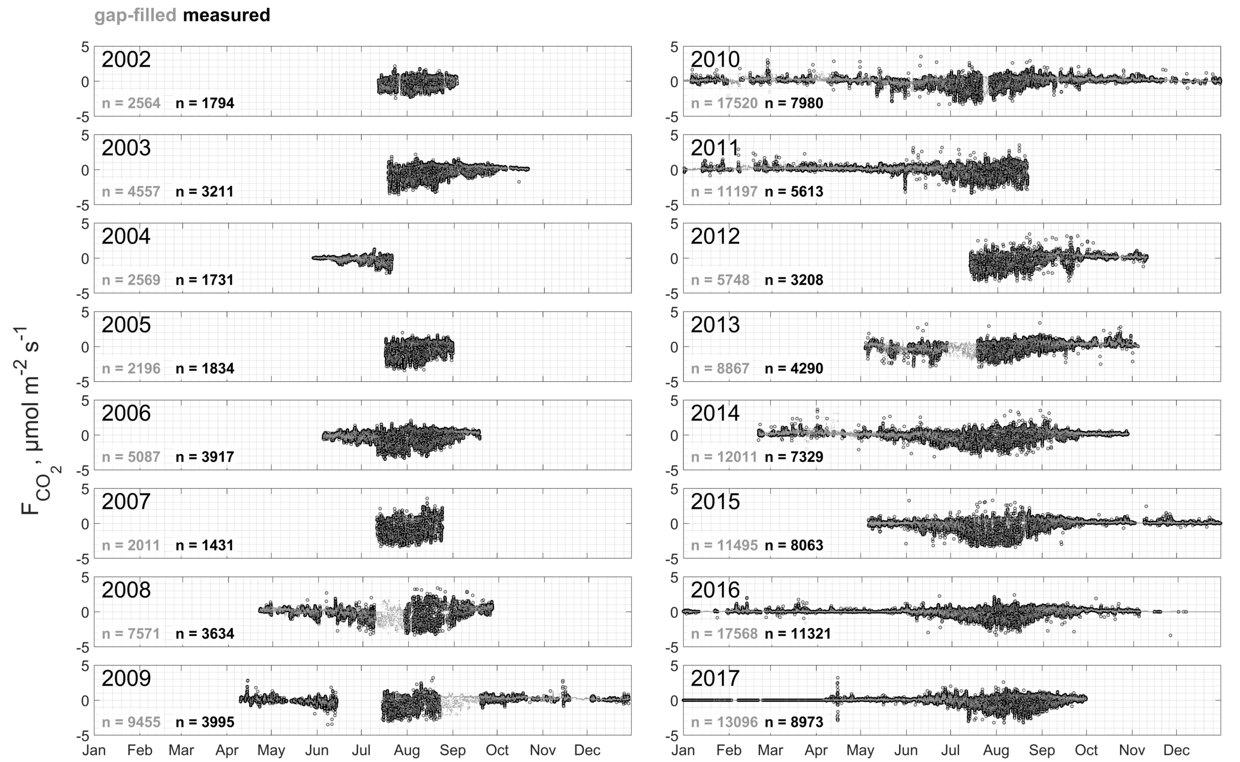

Figure 4. Multiannual carbon dioxide flux time series compiled from fluxes measured with closed-path and open-path sensors on Samoylov Island's river terrace. Fluxes of quality class 2 are not shown. Self-heating errors in the OP dataset have been corrected for. Additionally, the result from gap filling this time series with the MDS method is shown. The given number of values for the gap-filled time series include measured fluxes.

of the FLUXNET2015 data set, which includes over 1500 site-years of data. The algorithm of Reichstein et al. (2005) combines a screening procedure of the available data for similar environmental conditions (look-up table steps) and the use of a MDV method (diurnal cycle steps) if a gap could not be filled within the look-up table steps. Both techniques include moving windows with variable sizes that are increased until a solution can be found. Large gaps are skipped. To run the gap filling algorithm, we used the REddyProc routine that is accessible through a web-based service hosted by the Department of Biogeochemical Integration at Max Planck Institute Jena. The R-routine that is executed on this server is a further-developed and extended version of the Reichstein et al. (2005) approach and is described by Wutzler et al. (2017). We did not use the friction velocity filter or the flux partitioning capabilities of the REddy Proc online tool. Gap filling resulted in 131,908 ~~datapoints~~data points. The provided data set includes quality flags for each gap-filled value that depend on the used method and time window size, as defined by Reichstein et al. (2005). These flags take values between 0 and 3, with 0 denoting measurement data, 1 indicating most reliable and 3 least reliable gap-filled fluxes. To assess the overall quality of the gap filling result, the MDS algorithm, in a stepwise manner, treats single available values as gaps and fills them according to the described scheme. Pearson's correlation coefficient between our compiled CO_2 flux time series and the MDS quality assessment run, where these values were treated as artificial gaps, is 0.92, with a root mean squared error of 0.31 $\mu mol\, m^{-2}\, s^{-1}$.

3.6 Flux uncertainty estimation

Flux uncertainty can be regarded as a combination of a systematic and a random part. While the attempt should be made to remove systematic biases, random errors cannot be corrected for (Richardson et al., 2012). However, statistical methods exist to estimate the uncertainty of a flux measurement due to random errors. We used three different approaches from literature to quantify random uncertainty and addressed fluxes with a suspected large bias by correcting for it during processing or by filtering in the course of quality assessment.

Most importantly, systematic errors are introduced when underlying EC assumptions are not met. Using the method of Mauder and Foken (2004) that combines an assessment of well developed turbulence and steady state conditions, we identified biased fluxes and flagged them. Other sources of systematic errors that we addressed include for example the angle of attack correction of faulty sonic anemometer readings, filtering for low instrument signal strength, the OP self-heating correction and compensations for high frequency loss and air density fluctuations (see sections 3.2.2, 3.3 and 3.4). Although we are confident that we applied corrections for systematic errors both rigorously and carefully enough, biases were certainly not always removed efficiently. The quality flags included in the data set, reflect a level of confidence based on the assessment of general EC assumptions and our six additional quality filtering steps (see section 3.3).

To be able to include a random uncertainty estimate for each individual OP and CP flux in the provided data set, we set EddyPro to calculate random uncertainty estimates following Finkelstein and Sims (2001). The authors developed a method that aims at quantifying flux uncertainty associated with turbulence sampling errors. These errors can contribute largely to the total random error as they refer to the insufficient sampling of large eddies with high spectral energy. Due to the stochastic nature of turbulence, this type of error is random. To estimate its magnitude, the so-called integral turbulence time scale (ITS) is first determined by expressing the covariance of vertical wind velocity and gas concentration as a function of a lag time between these two time series. The ITS is then given by integrating the cross-correlation function theoretically from 0 to infinity, in practice, however, until an upper lag time limit is reached. The upper limit can be defined in three different ways in EddyPro. We used the definition of the normalized cross-correlation function reaching a value of $1/e = 0.369$ to determine an upper lag time limit used for integration. While the normalized cross-correlation should reach zero with increasing lag time in theory, in practice it sometimes does not. The setting we used on the one hand provides the least conservative estimate of the ITS but on the other hand offers computational efficiency and makes sure that an upper limit for integration can reliably be found. With the ITS, a flux uncertainty can be determined by calculating the variance of an EC flux or, as Finkelstein and Sims (2001) put it, by calculating the variance of the covariance. This ensemble variance would approach zero with the averaging time approaching infinity. In the data set available for download, a random uncertainty estimate calculated with the method of Finkelstein and Sims (2001) is given for each OP and CP flux (see Table 7). Random uncertainties based on ITS estimation observations increase with absolute fluxes with mean values of 0.16 and 0.05 $\mu mol\, m^{-2}\, s^{-1}$ for OP and CP fluxes (see Figure 5). OP random uncertainty estimates are generally larger and more scattered with respect to the corresponding flux values.

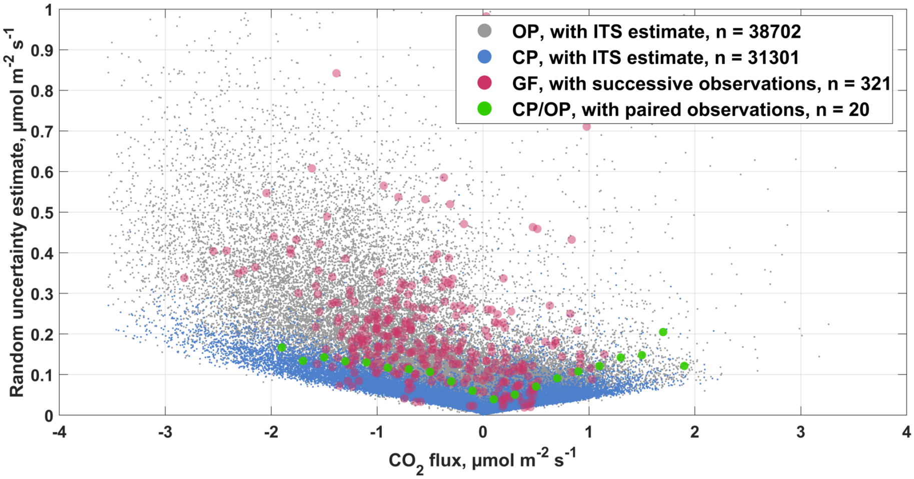

Figure 5. Random uncertainty estimates for all closed path (CP) and open-path (OP) CO_2 fluxes calculated using (1) estimates of the integral turbulence time scale (ITS), (2) the successive observations approach and results from gap filling (GF) and (3) the paired observations approach during periods with simultaneous OP and CP records.

As the above described random uncertainty estimate specifically addresses the turbulence sampling error, other sources of random flux errors such as the noise introduced by the different components of the measurement system are neglected. With simultaneous measurements from two sensors, we could additionally estimate random errors for the measurement system as a whole during times when the data sets from both sensors overlapped. We followed the paired observations approach as presented by Dragoni et al. (2007) and calculated a random error estimate ϵ as

$$\epsilon = \frac{1}{\sqrt{2}} \cdot (F_{CP} - F_{OP}) \quad (4)$$

with the closed-path and open-path CO_2 fluxes F_{CP} and F_{OP} of quality classes 0 and 1 in $\mu\text{mol}\,\text{m}^{-2}\,\text{s}^{-1}$. The distribution of ϵ estimates is shown in Figure 6. The ϵ values calculated with OP fluxes corrected for the self-heating error have a mean close to zero and are distributed more symmetrically than the ϵ values calculated with uncorrected OP fluxes. The mean of this distribution is shifted from its mode as well as from zero, indicating a much stronger systematic component whithin the measurement error. This result increases our confidence that the OP self-heating correction we applied was successful in removing a systematic bias from the data. Further following Dragoni et al. (2007), we used the ϵ system error data set from the overlap period to generate flux uncertainty estimates for bins of increasing OP flux ranges. We sorted the ϵ values in 20 corresponding flux bins between -2 and 2 $\mu\text{mol}\,\text{m}^{-2}\,\text{s}^{-1}$ and calculated an uncertainty estimate for each bin $\sigma(\epsilon)_i$ as

$$\sigma(\epsilon)_i = \sqrt{2}\frac{1}{N_j}\sum_{j=0}^{N_j} |\epsilon_{i,j} - \overline{\epsilon}_i| \quad (5)$$

Results show (see Figure 5) a similar data range and pattern of uncertainty estimates in relation to associated fluxes like the half-hourly values calculated after Finkelstein and Sims (2001).

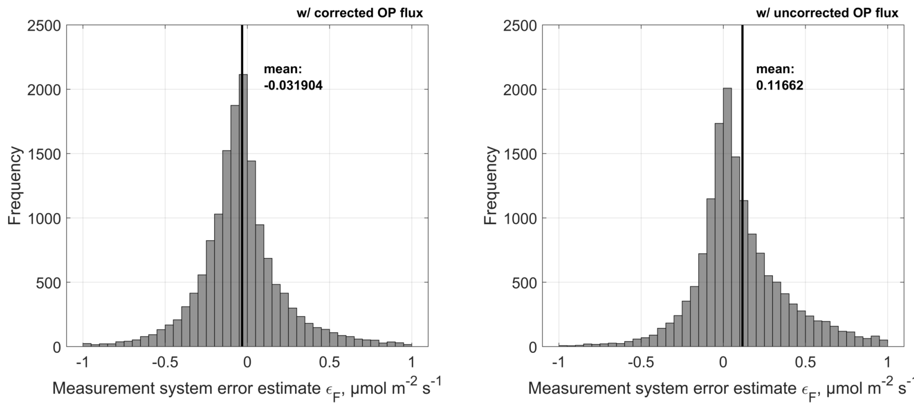

Figure 6. Distributions of the measurement system errors ϵ estimated using the paired observations approch for differences between closed path and corrected (left panel) as well as uncorrected (right panel) open-path (OP) fluxes.

As a third method of random uncertainty estimation we simplified the successive observations approach from Richardson et al. (2006) by using results of the quality run performed during MDS gap filling (see section 3.5). We selected the time steps when an flux observation and a MDS value that was estimated using a one day window and the MDV technique were available. We used the standard deviation of the fluxes measured at the same hour of day within a one day window, as an uncertainty estimate of the observed flux. Results are shown in Figure 5 and also increase with rising absolute fluxes in the same ranges as random uncertainties due to turbulence sampling error or measurement system error do.

We included the results obtained with ITS estimation into the uploaded data set considering the similarity between the uncertainty–flux relations calculated with independent methods as well as due to the advantage of a distinct uncertainty estimate for each sensor and time step.

3.7 Footprint modeling

In order to quantify the cumulative contribution of distinct surface classes to the EC source area, we evaluated the two-dimensional analytical footprint formulation described by Kormann and Meixner (2001) in combination with a $0.14\,\mathrm{m} \times 0.14\,\mathrm{m}$ resolution surface classification of Samoylov Island's central river terrace provided by Muster et al. (2012). The authors divide the surface into four classes based on hydrology and vegetation communities, as illustrated in Fig. Figure 2. Kormann and Meixner (2001) presented an analytical solution to the crosswind-distributed advection-diffusion equation described by Van Ulden (1978) and Horst and Weil (1992). Using the analytical model of Huang (1979), the authors solved the power-law profiles of horizontal wind velocity speed and eddy diffusivity by relating them to the Monin-Obukhov similarity theory, including the stability dependence of the exponents in the power laws at a certain height. We implemented the equations given in Kormann and Meixner (2001) as a Matlab (v. 9.2) function and added a quality filter, omitting calculations when friction velocity was larger than 0.9 $\mathrm{m\,s^{-1}}$ or smaller than 0 $\mathrm{m\,s^{-1}}$, wind speed was below zero or above 20 $\mathrm{m\,s^{-1}}$, the crosswind standard deviation was below zero or above 3 $\mathrm{m\,s^{-1}}$ or Monin-Obukhov length was smaller than 10^{-3} m or larger than 10^4

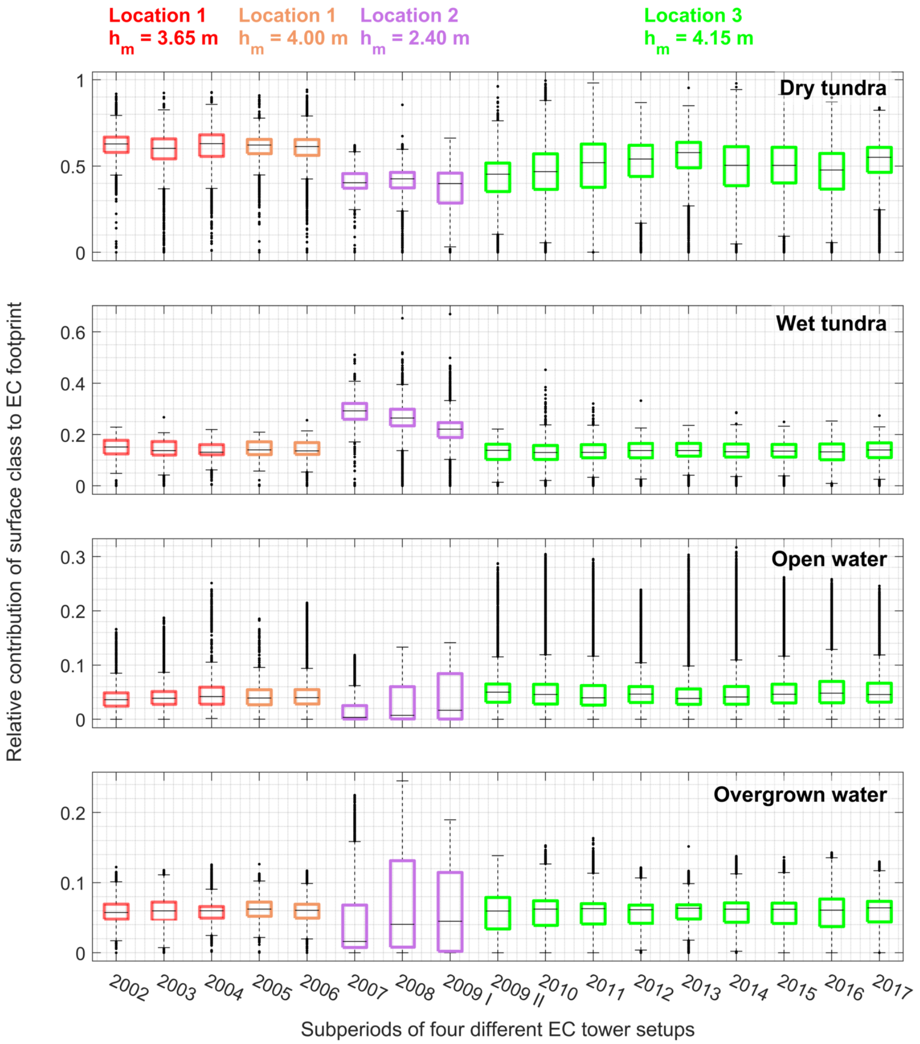

Figure 7. Mean surface class composition of the eddy covariance footprint during 17 subperiods of four different tower setups at three locations on Samoylov Island.

m. Prior to half-hourly footprint calculations, we additionally determined roughness length statistics for annual subsets of data and binned them in 2 ° wind direction classes. The medians of these classes were used in the subsequent half-hourly footprint estimation, depending on the mean wind direction during these 30 minutes. We evaluated the footprint model at the same resolution that was used by (Muster et al., 2012) to classify the surface (i. e. 0.14 m $\times$ 0.14 m). We could thereafter assign a probability of being the EC source area to each classified pixel and sum up the probabilities of all pixels belonging to the same surface class to estimate the contribution of each class. This proceeding to combine an EC source area estimation with a land cover classification is similar to what has been applied and described in more detail by Forbrich et al. (2011).

4 Discussion

Although we did our best to ensure the consistency and appropriateness of the data processing workflow for the presented NEE time series, due to technical and logistical constraints during 16 years of field work, disparities in the experimental setup exist which may challenge its integrity. The EC tower was relocated twice, the measurement height was changed three times (see Figure 2 and Table 1). These changes of tower location and measurement height affected the source area and hence the surface types sampled during flux measurements. Most notably, between July 2007 and June 2009, the EC tower was placed about 650 m south-west of its original position at the center of Samoylov Island, in an area with an increased coverage of the surface class *wet tundra*. This is revealed by the footprint analysis (Figure 6). While the EC footprint is dominated by the surface class *dry tundra* throughout the time series, during subperiods 2007, 2008 and 2009 I the contributions of *wet tundra* to the measured flux are significantly higher. To check the effect of the shifts in tower location and measurement height on cumulative CO_2-C fluxes, we calculated flux sums for a period when flux time series without gaps were available in most years. The overlapping period covers days of year 200 to 234, i.e. part of the growing season in all years except for 2004 (see Figure 8). Interannual variability of cumulative C fluxes in years with constant tower location (and measurement height) appears to be large and driven by a more complex set of variables than shifts in surface class contributions only. Flux sums from the periods when EC tower relocation led to a significant shift in EC footprint composition are well within the range of the distribution of cumulated fluxes from years with a more homogeneous EC fetch area. We therefore assume that, at least with respect to budget calculations, the presented long-term time series is not disrupted and can be regarded as representative for a polygonal tundra site dominated by *dry tundra*. For a more in depth analysis of flux dynamics, footprint information should and can be considered by users of the data set. Recently, a comparison between surface class level NEE models based on chamber measurements with EC fluxes, using the half-hourly footprint information provided in this data set for scaling, yielded good agreement between the results obtained with both methods (Eckhardt et al., 2018). We regard the availability of half-hourly footprint information in the presented NEE data set an attribute that sets it apart from other studies and holds chances for comprehensive analyses.

Apart from the changes in anemometer height, other deviations of the general instrument setup occurred due to limitations in data storage during two winter periods when the acquisition frequency was reduced to 5 Hz and 10 Hz respectively. Rinne et al. (2008) demonstrated in a field experiment that fluxes calculated from raw data recorded at frequencies below 20 Hz compare well with fluxes derived from high frequency raw data. Differences arise as an increase of random noise and not as a systematic bias. High frequency noise removal before ensemble spectra estimation in EddyPro is effective in limiting the effect of increased noise on the quality of transfer function estimation in the process of spectral correction. Overall spectral correction in EddyPro is expressed as a spectral correction factor (SCF) which comprises the effect of all applied compensations for high and low frequency loss. Raw fluxes are multiplied with the respective SCFs during processing. We compared the SCF distributions of the two above mentioned winter periods with statistics of the remaining parts of the time series when data was recorded at 20 Hz. SCF deviations between the different acquisition frequencies are minor (see Figure 9) what implies that systematic differences between fluxes calculated from raw data of different temporal resolutions are in fact small; random uncertainties increase, however.

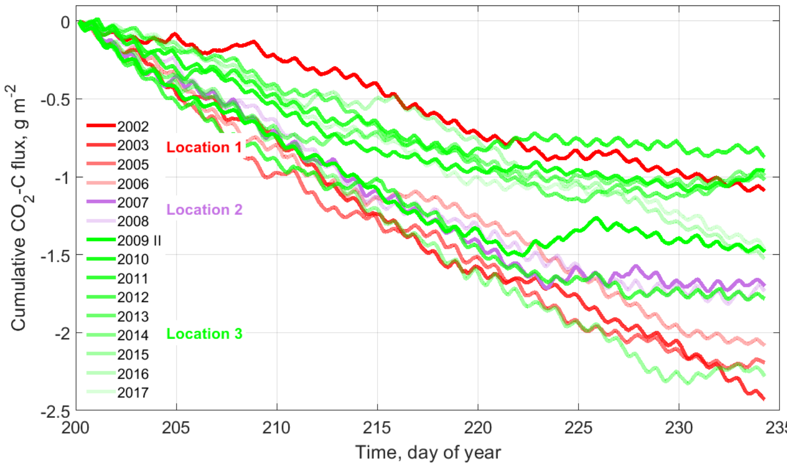

Figure 8. Comparison of cumulative CO_2 flux sums of different years during the same day of year range.

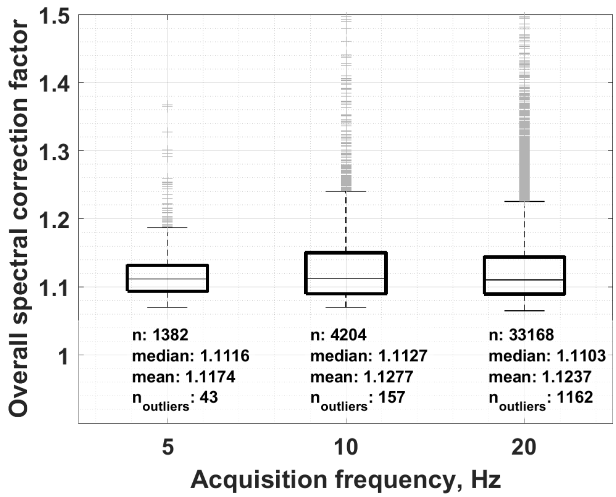

Figure 9. Spectral correction factor statistics for periods with different acquisition frequencies.

5 Scientific overview

While results on methane exchange fluxes and the soils' methane production and oxidation potential are more prominent in the publication record (e.g. Wagner et al., 2003; Kutzbach et al., 2004; Liebner and Wagner, 2007; Knoblauch et al., 2008; Sachs et al., 2008; , literature on CO_2 flux time series recorded with the same measurement system presented in this publication is available for distinct years. Flux processing has, however, been streamlined only now. The length of the time series, the addition of detailed footprint information, the site-specific correction of OP fluxes and the coherent processing and quality filtering distinguishes the data set at hand from past publications like the contribution made to the FLUXNET2015 data set (Kutzbach et al., 2015).

Ongoing analysis of the long-term data set (Kutzbach, unpublished) *inter alia* confirms what has been found in the past (Kutzbach, 2006; Kutzbach et al., 2007; Runkle et al., 2013). The polygonal tundra of Samoylov Island appears to be a robust growing season CO_2-C sink whereas this sink strength can vary that much interannually that prolonged low-level respiratory CO_2-C loss during the cold season can offset CO_2-C uptake during the vegetation period. Reduced summer uptake has been observed for both the coldest and warmest summers. Runkle et al. (2013) found that with frequent early season heat spells, the temperature-induced increase in respiratory release can exceed the rise in photosynthetic uptake. Recently, all data from this publication has been contributed to the Arctic Data Center's chamber and EC synthesis project *Reconciling historical and contemporary trends in terrestrial carbon exchange of the northern permafrost-zone* that aims at identifying seasonal and interannual C flux dynamics and its drivers based on a newly established pan-arctic data base.

In context with the improvement of earth system models (ESMs), carbon dioxide fluxes from Samylov Island can be especially of use due to the site's comparably high moss cover. Using data from Samoylov, Chadburn et al. (2017) found that current ESMs miss an observed early season CO_2 uptake peak suspected to be connected to the earlier onset of moss photosynthesis in comparison with vascular plants. Although there have been advances and e. g. Porada et al. (2013) developed a dynamic moss model for JSBACH (Raddatz et al., 2007), Chadburn et al. (2017) noted that the simulated CO_2 uptake and release terms combining vascular vegetation and moss carbon fluxes did not agree with observational data. The fact that the Samoylov Island NEE data set has now been extended and its quality has been greatly improved holds the opportunity to estimate the performance of updated ESM versions that are set up to represent carbon fluxes in the moss layer better.

6 Data availability

The data set was uploaded to the Pangaea data base (Holl and Kutzbach, 2018) and can be accessed through https://doi.pangaea.de/10.1594/PANGAEA.892751. The included columns are given in Table 7. Ancillary long-term time series of meteorological and soil variables from Samoylov Island are available from Boike et al. (2018) and can be accessed through https://doi.pangaea.de/10.1594/PANGAEA.891142.

7 Conclusions

We are confident that the presented carbon dioxide land–atmosphere flux data set is of high quality and is likely to be of value to the scientific community. We screened the data carefully and applied filtering rules to identify erroneous data, taking into account sensor diagnostics, time lag statistics and the presence of atmospheric conditions that allow for a robust application of the EC method. We followed standardized processing and quality control/assurance routines to allow for comparability between different years from our site as well as with flux time series from other tundra environments. With OP measurements being paralleled by CP measurements in seven years, we had the opportunity to correct for self-heating errors in our OP measurements with a site-specifically scaled correction term, rather than using default correction methods (e. g. Burba et al., 2008). We could therefore address different sensor setups with different correction terms and thereby improve our OP data set, as the self-heating effect has distinct impacts on sensors installed at different inclinations. We quantified the contribution of certain soil and vegetation community types to each half-hourly EC footprint, taking into account varying roughness lengths throughout different years and wind direction sectors. We estimated the cumulative probability of being the EC source area for the four main surface classes on Samoylov Islands' river terrace by using a classified image and by computing an analytical footprint model. Multiannual results show (see Table 6) that on average the combination of different surface classes within the EC footprint is representative for the surface composition of the whole river terrace that developed as a polygonal tundra landscape. According to Muster et al. (2012) the river terrace is composed of 65 % *dry tundra*, 19 % *wet tundra* and 16 % ponds (sum of *open water* and *overgrown*). On average, the surface class compositions within the EC footprint are very similar to these values. Deviations arise, however, in the years between 2007 and 2009, when the tower location was shifted from the center towards the south-western cliff of Samoylov Island. Nevertheless, the contributions of each surface class to the EC footprint are not only available on average, as presented in Table 6, but half-hourly in the uploaded data set, ensuring that EC source area deviations are quantifiable by a potential user. 16 years of consistently processed and quality-controlled carbon dioxide fluxes from a polygonal tundra landscape typical for Arctic lowlands are a valuable addition to the already existing data base of CO_2 net ecosystem exchange observations from the Arctic, especially because of the site's location in Northern Siberia, from where only limited data is available up to now. Furthermore, analysis of this NEE time series is not limited to the gas flux data only. An extensive data stream of meteorological and soil variables between 2002 and 2017 has recently been published by Boike et al. (2018). The authors made their records publicly accessible on the two long-term repositories Pangaea (https://doi.pangaea.de/10.1594/PANGAEA.891142) and Zenodo (https://zenodo.org/record/2223709). The fact of parallelly available ancillary ecosystem variables enables a potential user to put the gas flux dynamics reported in this publication into context with the variability of other ecosystem properties and potential flux drivers. We regard this type of analysis as vital to understand inter-annual variability of gas fluxes and are working on it ourselves (Kutzbach, unpublished).

Competing interests. No competing interests are present.

Acknowledgements. Without the dedicated work of many scientists, logistics experts and engineers over the years, we would not have been able to present this long-term eddy covariance NEE data set. We want to thank Niko Bornemann, Tim Eckhardt, Mauel Helbig, Lars Heling, Oliver Kaufmann, Zoé Rehder, Norman Rößger, Norman Rüggen, Günter Stoof and Waldemar Schneider for their commitment, diligence and ingenuity. We thank Jakob Sievers for providing us with a starting point for the Matlab implementation of the Kormann and Meixner (2001) footprint model and Norman R¨oßger for sharing his analysis of the long-term meteorological data from Tiksi with us. This work was supported through the Cluster of Excellence CliSAP (EXC177), Universität Hamburg, funded through the German Science Foundation (DFG), by the European Commission through the project PAGE21 (FP7-ENV-2011, 282700) and by the German Ministry of Education and Research (BMBF) through the projects CarboPerm (03G0836A) and KoPf (03F0764A).

References

AARI: Electronic archive Arctic and Antarctic Research Institute long-term meteorological and upper-air observations Hydrometeorological Observatory Tiksi for 1932 - 2017, http://www.aari.ru/resources/d0024/archive/description_e.html, accessed: 2018/09/08, 2018.

Antonov, V.: The Lena river delta, Hydrometeoizdat, Leningrad, USSR, 1967.

Aubinet, M., Vesala, T., and Papale, D.: Eddy covariance: a practical guide to measurement and data analysis, Springer, 2012.

Baldocchi, D., Chu, H., and Reichstein, M.: Inter-annual variability of net and gross ecosystem carbon fluxes: A review, Agricultural and Forest Meteorology, 2017.

Boike, J., Wille, C., and Abnizova, A.: Climatology and summer energy and water balance of polygonal tundra in the Lena River Delta, Siberia, Journal of Geophysical Research: Biogeosciences, 113, 1–15, 2008.

Boike, J., Grüber, M., Langer, M., Piel, K., and Scheritz, M.: Orthomosaic Samoylov Island, Lena Delta, Siberia, https://doi.org/10.1594/PANGAEA.786073, 2012.

Boike, J., Kattenstroth, B., Abramova, K., Bornemann, N., Chetverova, A., Fedorova, I., Fröb, K., Grigoriev, M., Grüber, M., Kutzbach, L., Langer, M., Minke, M., Muster, S., Piel, K., Pfeiffer, E. M., Stoof, G., Westermann, S., Wischnewski, K., Wille, C., and Hubberten, H. W.: Baseline characteristics of climate, permafrost and land cover from a new permafrost observatory in the Lena River Delta, Siberia (1998-2011), Biogeosciences, 10, 2105–2128, 2013.

Boike, J., Nitzbon, J., Anders, K., Grigoriev, M., Bolshiyanov, D., Langer, M., Lange, S., Bornemann, N., Morgenstern, A., Schreiber, P., Wille, C., Chadburn, S., Gouttevin, I., and Kutzbach, L.: A 16-year record (2002–2017) of permafrost, active layer, and meteorological conditions at the Samoylov Island Arctic permafrost research site, Lena River Delta, northern Siberia: an opportunity to validate remote sensing data and land surface, snow, and permafrost models, Earth System Science Data Discussions, 2018, 1–77, 2018.

Bolshiyanov, D., Makarov, A., and Savelieva, L.: Lena River delta formation during the Holocene, Biogeosciences, 12, 579–593, 2015.

Brown, J., Ferrians Jr, O., Heginbottom, J., and Melnikov, E.: Circum-Arctic map of permafrost and ground-ice conditions, US Geological Survey Reston, 1997.

Burba, G., Schmidt, A., Scott, R. L., Nakai, T., Kathilankal, J., Fratini, G., Hanson, C., Law, B., McDermitt, D. K., Eckles, R., et al.: Calculating CO2 and H2O eddy covariance fluxes from an enclosed gas analyzer using an instantaneous mixing ratio, Global Change Biology, 18, 385–399, 2012.

Burba, G. G., Anderson, D. J., Xu, L., and McDermitt, D. K.: Correcting apparent off-season CO2 uptake due to surface heating of an open path gas analyzer: progress report of an ongoing study, in: Proceedings of 27th Annual Conference of Agricultural and Forest Meteorology, San Diego, California, 13pp, 2006.

Burba, G. G., McDermitt, D. K., Grelle, A., Anderson, D. J., and Xu, L.: Addressing the influence of instrument surface heat exchange on the measurements of CO_2 flux from open-path gas analyzers, Global Change Biology, 14, 1854–1876, 2008.

Chadburn, S. E., Krinner, G., Porada, P., Bartsch, A., Beer, C., Belelli Marchesini, L., Boike, J., Ekici, A., Elberling, B., Friborg, T., Hugelius, G., Johansson, M., Kuhry, P., Kutzbach, L., Langer, M., Lund, M., Parmentier, F.-J. W., Peng, S., Van Huissteden, K., Wang, T., Westermann, S., Zhu, D., and Burke, E. J.: Carbon stocks and fluxes in the high latitudes: using site-level data to evaluate Earth system models, Biogeosciences, 14, 5143–5169, 2017.

Davidson, E. A. and Janssens, I. A.: Temperature sensitivity of soil carbon decomposition and feedbacks to climate change, Nature, 440, 165, 2006.

Dragoni, D., Schmid, H. P., Grimmond, C. S. B., and Loescher, H. W.: Uncertainty of annual net ecosystem productivity estimated using eddy covariance flux measurements, Journal of Geophysical Research: Atmospheres, 112, 2007.

Eckhardt, T., Knoblauch, C., Kutzbach, L., Simpson, G., Abakumov, E., and Pfeiffer, E.-M.: Partitioning CO_2 net ecosystem exchange fluxes on the microsite scale in the Lena River Delta, Siberia, Biogeosciences Discussions, 2018, 1–27, in review, 2018.

Ekici, A., Beer, C., Hagemann, S., and Hauck, C.: Simulating high-latitude permafrost regions by the JSBACH terrestrial ecosystem model, Geoscientific Model Development, 7, 631–647, 2014.

Falge, E., Baldocchi, D., Olson, R., Anthoni, P., Aubinet, M., Bernhofer, C., Burba, G., Ceulemans, R., Clement, R., Dolman, H., Granier, A., Gross, P., Grünwald, T., Hollinger, D., Jensen, N.-O., Katul, G., Keronen, P., Kowalski, A., Lai, C. T., Law, B. E., Meyers, T., Moncrieff, J., Moors, E., Munger, J., Pilegaard, K., Rannik, Ü., Rebmann, C., Suyker, A., Tenhunen, J., Tu, K., Verma, S., Vesala, T., Wilson, K., and Wofsy, S.: Gap filling strategies for defensible annual sums of net ecosystem exchange, Agricultural and Forest Meteorology, 107, 43 – 69, 2001.

Fan, S.-M., Wofsy, S. C., Bakwin, P. S., Jacob, D. J., and Fitzjarrald, D. R.: Atmosphere-biosphere exchange of CO2 and O3 in the central Amazon forest, Journal of Geophysical Research: Atmospheres, 95, 16 851–16 864, 1990.

Fedorova, I., Chetverova, A., Bolshiyanov, D., Makarov, A., Boike, J., Heim, B., Morgenstern, A., Overduin, P. P., Wegner, C., Kashina, V., Eulenburg, A., Dobrotina, E., and Sidorina, I.: Lena Delta hydrology and geochemistry: long-term hydrological data and recent field observations, Biogeosciences, 12, 345–363, 2015.

Finkelstein, P. L. and Sims, P. F.: Sampling error in eddy correlation flux measurements, Journal of Geophysical Research, 106, 3503, 2001.

Forbrich, I., Kutzbach, L., Wille, C., Becker, T., Wu, J., and Wilmking, M.: Cross-evaluation of measurements of peatland methane emissions on microform and ecosystem scales using high-resolution landcover classification and source weight modelling, Agricultural and forest meteorology, 151, 864–874, 2011.

Gash, J. H. C. and Culf, a. D.: Applying a linear detrend to eddy correlation data in realtime, Boundary-Layer Meteorology, 79, 301 – 306, 1996.

Grigoriev, M.: *Kriomorfogenez ust'evoy oblasti r. Leny* (Cryomorphogenesis in the Lena Delta (in Russian)), Permafrost Institute Press, Yakutsk, 1993.

Helbig, M., Boike, J., Langer, M., Schreiber, P., Runkle, B., and Kutzbach, L.: Spatial and seasonal variability of polygonal tundra water balance: Lena River Delta, northern Siberia (Russia), Hydrogeology Journal, 21, 133–147, 2013.

Holl, D. and Kutzbach, L.: A long-term (2002 to 2017) record of closed-path and open-path eddy covariance CO_2 net ecosystem exchange fluxes from the Siberian Arctic, https://doi.pangaea.de/10.1594/PANGAEA.892751, 2018.

Horst, T. and Weil, J.: Footprint estimation for scalar flux measurements in the atmospheric surface layer, Boundary-Layer Meteorology, 59, 279–296, 1992.

Horst, T. W. and Lenschow, D. H.: Attenuation of scalar fluxes measured with spatially-displaced sensors, Boundary-Layer Meteorology, 130, 275 – 300, 2009.

Huang, C.: A theory of dispersion in turbulent shear flow, Atmospheric Environment (1967), 13, 453–463, 1979.

Ibrom, A., Dellwik, E., Flyvbjerg, H., Jensen, N. O., and Pilegaard, K.: Strong low-pass filtering effects on water vapour flux measurements with closed-path eddy correlation systems, Agricultural and Forest Meteorology, 147, 140 – 156, 2007a.

Ibrom, A., Dellwik, E., Larsen, S. E., and Pilegaard, K.: On the use of the Webb–Pearman–Leuning theory for closed path eddy correlation measurements, Tellus B, 59, 937–946, 2007b.

IUSS Working Group WRB: World Reference Base for Soil Resources 2014, update 2015 International soil classification system for naming soils and creating legends for soil maps, World Soil Resources Reports No. 106, p. 192, 2015.

Järvi, L., Mammarella, I., Eugster, W., Ibrom, A., Siivola, E., Dellwik, E., Keronen, P., Burba, G., and Vesala, T.: Comparison of net CO_2 fluxes measured with open-and closed-path infrared gas analyzers in an urban complex environment., Boreal Environment Research, 14, 2009.

Kaimal, J. and Finnigan, J.: Atmospheric Boundary Layer Flows: Their structure and measurements, Oxford University Press, Oxford, 1994.

Kaiser, S., Göckede, M., Castro-Morales, K., Knoblauch, C., Ekici, A., Kleinen, T., Zubrzycki, S., Sachs, T., Wille, C., and Beer, C.: Process-based modelling of the methane balance in periglacial landscapes (JSBACH-methane), Geoscientific Model Development, 10, 333–358, 2017.

Khvorostyanov, D., Krinner, G., Ciais, P., Heimann, M., and Zimov, S.: Vulnerability of permafrost carbon to global warming. Part I: model description and role of heat generated by organic matter decomposition, Tellus B, 60, 250–264, 2008.

Kittler, F., Eugster, W., Foken, T., Heimann, M., Kolle, O., and Göckede, M.: High-quality eddy covariance CO_2 budgets under cold climate conditions, Journal of Geophysical Research: Biogeosciences, 122, 2064–2084, 2017.

Knoblauch, C., Zimmermann, U., Blumenberg, M., Michaelis, W., and Pfeiffer, E.-M.: Methane turnover and temperature response of methane-oxidizing bacteria in permafrost-affected soils of northeast Siberia, Soil Biology and Biochemistry, 40, 3004–3013, 2008.

Knoblauch, C., Spott, O., Evgrafova, S., Kutzbach, L., and Pfeiffer, E.-M.: Regulation of methane production, oxidation, and emission by vascular plants and bryophytes in ponds of the northeast Siberian polygonal tundra, Journal of Geophysical Research: Biogeosciences, 120, 2525–2541, 2015.

Knoblauch, C., Beer, C., Liebner, S., Grigoriev, M. N., and Pfeiffer, E.-M.: Methane production as key to the greenhouse gas budget of thawing permafrost, Nature Climate Change, 8, 309, 2018.

Kormann, R. and Meixner, F. X.: An analytical footprint model for non-neutral stratification, Boundary-Layer Meteorology, 99, 207 – 224, 2001.

Koven, C. D., Ringeval, B., Friedlingstein, P., Ciais, P., Cadule, P., Khvorostyanov, D., Krinner, G., and Tarnocai, C.: Permafrost carbon-climate feedbacks accelerate global warming, Proceedings of the National Academy of Sciences, 108, 14 769–14 774, 2011.

Kutzbach, L.: The exchange of energy, water and carbon dioxide between wet arctic tundra and the atmosphere at the Lena River Delta, Northern Siberia, Berichte zur Polar-und Meeresforschung (Reports on Polar and Marine Research), 541, 2006.

Kutzbach, L., Wagner, D., and Pfeiffer, E.-M.: Effect of microrelief and vegetation on methane emission from wet polygonal tundra, Lena Delta, Northern Siberia, Biogeochemistry, 69, 341–362, 2004.

Kutzbach, L., Wille, C., and Pfeiffer, E. M.: The exchange of carbon dioxide between wet arctic tundra and the atmosphere at the Lena River Delta, Northern Siberia, Biogeosciences, 4, 869–890, 2007.

Kutzbach, L., Sachs, T., Boike, J., Wille, C., Schreiber, P., Langer, M., and Pfeiffer, E.-M.: FLUXNET2015 RU-Sam Samoylov, Tech. rep., FluxNet; University of Hamburg; Alfred Wegener Institute; GFZ German Research Centre for Geosciences, https://doi.org/10.18140/FLX/1440185, 2015.

Langer, M., Westermann, S., Muster, S., Piel, K., and Boike, J.: The surface energy balance of a polygonal tundra site in northern Siberia Part 1: Spring to fall, The Cryosphere, 5, 151, 2011a.

Langer, M., Westermann, S., Muster, S., Piel, K., and Boike, J.: The surface energy balance of a polygonal tundra site in northern Siberia Part 2: Winter, Cryosphere, 5, 509–524, 2011b.

Liebner, S. and Wagner, D.: Abundance, distribution and potential activity of methane oxidizing bacteria in permafrost soils from the Lena Delta, Siberia, Environmental microbiology, 9, 107–117, 2007.

Liebner, S., Zeyer, J., Wagner, D., Schubert, C., Pfeiffer, E.-M., and Knoblauch, C.: Methane oxidation associated with submerged brown mosses reduces methane emissions from Siberian polygonal tundra, Journal of Ecology, 99, 914–922, 2011.

MacDougall, A. H., Avis, C. A., and Weaver, A. J.: Significant contribution to climate warming from the permafrost carbon feedback, Nature Geoscience, 5, 719, 2012.

Mauder, M. and Foken, T.: Documentation and instruction manual of the eddy covariance software package TK2, Univ, Arbeitsergebnisse, Universität Bayreuth, Abt. Mikrometeorologie, 26, 45, 2004.

McGuire, A. D., Christensen, T. R., Hayes, D., Heroult, A., Euskirchen, E., Kimball, J. S., Koven, C., Lafleur, P., Miller, P. A., Oechel, W., Peylin, P., Williams, M., and Yi, Y.: An assessment of the carbon balance of Arctic tundra: comparisons among observations, process models, and atmospheric inversions, Biogeosciences, 9, 3185–3204, 2012.

McGuire, A. D., Lawrence, D. M., Koven, C., Clein, J. S., Burke, E., Chen, G., Jafarov, E., MacDougall, A. H., Marchenko, S., Nicolsky, D., et al.: Dependence of the evolution of carbon dynamics in the northern permafrost region on the trajectory of climate change, Proceedings of the National Academy of Sciences, p. 201719903, 2018.

Moffat, A. M., Papale, D., Reichstein, M., Hollinger, D. Y., Richardson, A. D., Barr, A. G., Beckstein, C., Braswell, B. H., Churkina, G., Desai, A. R., Falge, E., Gove, J. H., Heimann, M., Hui, D., Jarvis, A. J., Kattge, J., Noormets, A., and Stauch, V. J.: Comprehensive comparison of gap-filling techniques for eddy covariance net carbon fluxes, Agricultural and Forest Meteorology, 147, 209 – 232, 2007.

Moncrieff, J., Valentini, R., Greco, S., Guenther, S., and Ciccioli, P.: Trace gas exchange over terrestrial ecosystems: methods and perspectives in micrometeorology, Journal of Experimental Botany, 48, 1133 – 1142, 1997.

Moncrieff, J., Clement, R., Finnigan, J., and Meyers, T.: Averaging, detrending, and filtering of eddy covariance time series, in: Handbook of micrometeorology, edited by Lee, X., Massman, W., and Law, B., pp. 7–31, Springer Netherlands, Dordrecht, 2004.

Munger, J. W., Loescher, H. W., and Luo, H.: Measurement, tower, and site design considerations, in: Eddy Covariance: A Practical Guide to Measurement and Data Analysis, edited by Aubinet, M., Vesala, T., and Papale, D., pp. 21–58, Springer, 2012.

Muster, S., Langer, M., Heim, B., Westermann, S., and Boike, J.: Subpixel heterogeneity of ice-wedge polygonal tundra: a multi-scale analysis of land cover and evapotranspiration in the Lena River Delta, Siberia, Tellus B: Chemical and Physical Meteorology, 64, 17 301, 2012.

Nakai, T., Van der Molen, M., Gash, J., and Kodama, Y.: Correction of sonic anemometer angle of attack errors, Agricultural and Forest Meteorology, 136, 19–30, 2006.

Oechel, W. C., Laskowski, C. A., Burba, G., Gioli, B., and Kalhori, A. A. M.: Annual patterns and budget of CO2 flux in an Arctic tussock tundra ecosystem, Journal of Geophysical Research: Biogeosciences, 119, 323–339, 2014.

Park, T., Ganguly, S., Tømmervik, H., Euskirchen, E. S., Høgda, K.-A., Karlsen, S. R., Brovkin, V., Nemani, R. R., and Myneni, R. B.: Changes in growing season duration and productivity of northern vegetation inferred from long-term remote sensing data, Environmental Research Letters, 11, 084 001, 2016.

Pfeiffer, E.-M. and Grigoriev, M. N.: Russian-German Cooperation SYSTEM LAPTEV SEA 2000: The Expedition LENA 2001, Reports on Polar Research, 2002.

Porada, P., Weber, B., Elbert, W., Pöschl, U., and Kleidon, A.: Estimating global carbon uptake by lichens and bryophytes with a process-based model, Biogeosciences, 10, 6989–7033, 2013.

Raddatz, T., Reick, C., Knorr, W., Kattge, J., Roeckner, E., Schnur, R., Schnitzler, K.-G., Wetzel, P., and Jungclaus, J.: Will the tropical land biosphere dominate the climate–carbon cycle feedback during the twenty-first century?, Climate Dynamics, 29, 565–574, 2007.

Reichstein, M., Falge, E., Baldocchi, D., Papale, D., Aubinet, M., Berbigier, P., Bernhofer, C., Buchmann, N., Gilmanov, T., Granier, A., Grunwald, T., Havrankova, K., Ilvesniemi, H., Janous, D., Knohl, A., Laurila, T., Lohila, A., Loustau, D., Matteucci, G., Meyers, T., Miglietta, F., Ourcival, J.-M., Pumpanen, J., Rambal, S., Rotenberg, E., Sanz, M., Tenhunen, J., Seufert, G., Vaccari, F., Vesala, T., Yakir, D., and Valentini, R.: On the separation of net ecosystem exchange into assimilation and ecosystem respiration: review and improved algorithm, Global Change Biology, 11, 1424 – 1439, 2005.

Richardson, A. D., Hollinger, D. Y., Burba, G. G., Davis, K. J., Flanagan, L. B., Katul, G. G., Munger, J. W., Ricciuto, D. M., Stoy, P. C., Suyker, A. E., et al.: A multi-site analysis of random error in tower-based measurements of carbon and energy fluxes, Agricultural and Forest Meteorology, 136, 1–18, 2006.

Richardson, A. D., Aubinet, M., Barr, A. G., Hollinger, D. Y., Ibrom, A., Lasslop, G., and Reichstein, M.: Uncertainty quantification, in: Eddy Covariance: A Practical Guide to Measurement and Data Analysis, edited by Aubinet, M., Vesala, T., and Papale, D., pp. 173–209, Springer, 2012.

Rinne, J., Douffet, T., Prigent, Y., and Durand, P.: Field comparison of disjunct and conventional eddy covariance techniques for trace gas flux measurements, Environmental pollution, 152, 630–635, 2008.

Rogiers, N., Conen, F., Furger, M., Stöckli, R., and Eugster, W.: Impact of past and present land-management on the C-balance of a grassland in the Swiss Alps, Global Change Biology, 14, 2613–2625, 2008.

Romanovskii, N., Hubberten, H.-W., Gavrilov, A., Tumskoy, V., and Kholodov, A.: Permafrost of the east Siberian Arctic shelf and coastal lowlands, Quaternary Science Reviews, 23, 1359–1369, 2004.

Romanovsky, V. E., Smith, S. L., and Christiansen, H. H.: Permafrost thermal state in the polar Northern Hemisphere during the international polar year 2007–2009: a synthesis, Permafrost and Periglacial processes, 21, 106–116, 2010.

Runkle, B., Sachs, T., Wille, C., Pfeiffer, E.-M., and Kutzbach, L.: Bulk partitioning the growing season net ecosystem exchange of CO 2 in Siberian tundra reveals the seasonality of its carbon sequestration strength, Biogeosciences, 10, 1337–1349, 2013.

Runkle, B. R., Wille, C., Gažovič, M., and Kutzbach, L.: Attenuation correction procedures for water vapour fluxes from closed-path eddy-covariance systems, Boundary-layer meteorology, 142, 401–423, 2012.

Sachs, T., Wille, C., Boike, J., and Kutzbach, L.: Environmental controls on ecosystem-scale CH4 emission from polygonal tundra in the Lena River Delta, Siberia, Journal of Geophysical Research: Biogeosciences, 113, 2008.

Sachs, T., Giebels, M., Boike, J., and Kutzbach, L.: Environmental controls on CH4 emission from polygonal tundra on the microsite scale in the Lena river delta, Siberia, Global Change Biology, 16, 3096–3110, 2010.

Schneider, J., Grosse, G., and Wagner, D.: Land cover classification of tundra environments in the Arctic Lena Delta based on Landsat 7 ETM+ data and its application for upscaling of methane emissions, Remote Sensing of Environment, 113, 380–391, 2009.

Schneider von Deimling, T., Meinshausen, M., Levermann, A., Huber, V., Frieler, K., Lawrence, D., and Brovkin, V.: Estimating the near-surface permafrost-carbon feedback on global warming, Biogeosciences, 9, 649, 2012.

Schuur, E., Abbott, B., Bowden, W., Brovkin, V., Camill, P., Canadell, J., Chanton, J., Chapin, F., Christensen, T., Ciais, P., et al.: Expert assessment of vulnerability of permafrost carbon to climate change, Climatic Change, 119, 359–374, 2013.

Schuur, E., McGuire, A. D., Schädel, C., Grosse, G., Harden, J., Hayes, D., Hugelius, G., Koven, C., Kuhry, P., Lawrence, D., et al.: Climate change and the permafrost carbon feedback, Nature, 520, 171–179, 2015.

Schuur, E. A., Bockheim, J., Canadell, J. G., Euskirchen, E., Field, C. B., Goryachkin, S. V., Hagemann, S., Kuhry, P., Lafleur, P. M., Lee, H., et al.: Vulnerability of permafrost carbon to climate change: Implications for the global carbon cycle, AIBS Bulletin, 58, 701–714, 2008.

Schwamborn, G., Rachold, V., and Grigoriev, M. N.: Late Quaternary sedimentation history of the Lena Delta, Quaternary international, 89, 119–134, 2002.

Soil Survey Staff: Keys to Soil Taxonomy, Twevfth Edition, 2014.

Tarnocai, C., Canadell, J., Schuur, E., Kuhry, P., Mazhitova, G., and Zimov, S.: Soil organic carbon pools in the northern circumpolar permafrost region, Global biogeochemical cycles, 23, 2009.

Van Ulden, A.: Simple estimates for vertical diffusion from sources near the ground, Atmospheric Environment (1967), 12, 2125–2129, 1978.

Vickers, D. and Mahrt, L.: Quality control and flux sampling problems for tower and aircraft data, Journal of Atmospheric and Oceanic Technology, 14, 512 – 526, 1997.

Wagner, D., Kobabe, S., Pfeiffer, E.-M., and Hubberten, H.-W.: Microbial controls on methane fluxes from a polygonal tundra of the Lena Delta, Siberia, Permafrost and periglacial processes, 14, 173–185, 2003.

Walker, H. J.: Arctic deltas, Journal of Coastal Research, pp. 719–738, 1998.

Wania, R., Ross, I., and Prentice, I.: Integrating peatlands and permafrost into a dynamic global vegetation model: 2. Evaluation and sensitivity of vegetation and carbon cycle processes, Global Biogeochemical Cycles, 23, 2009a.

Wania, R., Ross, I., and Prentice, I. C.: Integrating peatlands and permafrost into a dynamic global vegetation model: 1. Evaluation and sensitivity of physical land surface processes, Global Biogeochemical Cycles, 23, 2009b.

Wania, R., Ross, I., and Prentice, I.: Implementation and evaluation of a new methane model within a dynamic global vegetation model: LPJ-WHyMe v1. 3.1, Geoscientific Model Development, 3, 565, 2010.

Webb, E. K., Pearman, G. I., and Leuning, R.: Correction of flux measurements for density effects due to heat and water vapour transfer, Quarterly Journal of the Royal Meteorological Society, 106, 85–100, 1980.

Wille, C., Kutzbach, L., Sachs, T., Wagner, D., and PFEIFFER, E.-M.: Methane emission from Siberian arctic polygonal tundra: eddy covariance measurements and modeling, Global Change Biology, 14, 1395–1408, 2008.

Wutzler, T., Moffat, A., Migliavacca, M., Knauer, J., Menzer, O., Sickel, K., and Reichstein, M.: Reddyproc: Enabling researchers to process eddy-covariance data, in: EGU General Assembly Conference Abstracts, vol. 19, p. 12954, 2017.

Yershov, E. D.: General geocryology, Cambridge University Press, 2004.

Zimov, S. A., Schuur, E. A., and Chapin, F. S.: Permafrost and the global carbon budget, Science, 312, 1612–1613, 2006.

Zona, D., X., X., Hufkens, K., Gioli, B., Burba, G., Goodrich, J. P., Liljedahl, A. K., Euskirchen, E. S., Watts, J. D., Kimball, J. S., Heimann, M., Goeckede, M., Kittler, F., Lund, M., Dolman, H., Belelli Marchesini, L., Commane, R. S., Wofsy, C., Miller, C. E., Lipson, D. A., Kalhori, K. A., Arndt, A., Kutzbach, L., Boike, J., Wille, C., Holl, D., Sachs, T., Song, X., Humphreys, E. R., Lafleur, P. M., Koven, C. D., and Oechel, W. C.: Pan-Arctic temperature response of tundra carbon sequestration across scales, in review.

Zubrzycki, S., Kutzbach, L., Grosse, G., Desyatkin, A., and Pfeiffer, E.-M.: Organic carbon and total nitrogen stocks in soils of the Lena River Delta, Biogeosciences, 10, 3507, 2013.

Table 1. List of deployed instrument types. All infrared gas analyzers were manufactured by LI-COR Biosciences (USA), R3 sonic anemometers were built by Gill Instruments Ltd. (UK), CSAT3 anomemeters by Campbell Scientific Ltd. (UK)

	Gas analyzer		Anemometer		Data coverage	
Year	**Closed path**	**Open path**	**Model**	**Height, m**	**Date range**	**Days**
2002	LI-7000	n/a	R3	3.65	12-Jul to 03-Sep	53
2003	LI-7000	n/a	R3	3.65	19-Jul to 22-Oct	95
2004	LI-7000	n/a	R3	3.65	28-May to 20-Jul	53
2005	LI-7000	n/a	R3	4	17-Jul to 01-Sep	46
2006	LI-7000	n/a	R3	4	05-Jun to 19-Sep	106
2007	n/a	LI-7500	CSAT3	2.4	11-Jul to 23-Aug	36
2008	n/a	LI-7500	CSAT3	2.4	22-Apr to 26-Sep	157
2009 I	n/a	LI-7500	CSAT3	2.4	10-Apr to 14-Jun	65
2009 II	n/a	LI-7500	CSAT3	4.15	15-Jul to 29-Dec	167
2010	LI-7000	LI-7500	CSAT3	4.15	01-Jan to 31-Dec	359
2011	LI-7000	LI-7500	CSAT3	4.15	01-Jan to 22-Aug	233
2012	n/a	LI-7500	CSAT3	4.15	13-Jul to 10-Nov	120
2013	LI-7000	LI-7500A	CSAT3	4.15	04-May to 05-Nov	185
2014	LI-7000	LI-7500A	CSAT3	4.15	21-Feb to 29-Oct	250
2015	LI-7000	LI-7500A	CSAT3	4.15	06-May to 31-Dec	239
2016	LI-7000	LI-7500A	CSAT3	4.15	01-Jan to 19-Nov	323
2017	LI-7000	LI-7500A	CSAT3	4.15	01-Jan to 30-Sep	272

~~Multiannual time series of the presented closed-path (black dots) and open-path (gray dots) flux datasets from Samoylov Island's river terrace. Fluxes of quality class 2 are not shown. Self-heating errors in the OP dataset have been corrected for.~~

~~Multiannual time series of the presented closed-path (black dots) and uncorrected open-path (gray dots) flux datasets from Samoylov Island's river terrace. Fluxes of quality class 2 are not shown.~~

Table 2. Eddy covariance flux processing steps. Partly differing processing was applied to raw data from closed and open-path analyzers. OP and CP fluxes were computed consistently for the whole period from 2002 to 2017. Setup-dependent statistics (for time lags and *in situ* spectral correction methods) were evaluated annually or if tower position, CP pump speed or any other analyzer metadata changed.

Processing step	**Method**	
	Closed path data	**Open path data**
Spike detection & removal	raw data spike removal (Vickers and Mahrt, 1997)	
Angle of attack correction	from 2002 to 2006 during Gill anemometer deployment (Nakai et al., 2006)	n/a, sensor was not deployed between 2002 and 2006
Axis rotation	Double rotation (Kaimal and Finnigan, 1994)	
Detrending	linear, (Gash and Culf, 1996)	
Correction for air density fluctuations	sample-wise conversion of raw data to mixing ratios (Ibrom et al., 2007b; Burba et al., 2012)	application of WPL-Terms to fluxes (Webb et al., 1980)
Time lag compensation	covariance maximization with nominal time lag from statistics	covariance maximization
Spectral corrections for		
High-pass filtering	analytic (Moncrieff et al., 2004)	
Low-pass filtering	*in situ*/analytic (Ibrom et al., 2007a)	analytic (Moncrieff et al., 1997)
Instrument separation	Horst and Lenschow (2009)	n/a
Eddy Pro version	$\geq$ 6.0.0	

Table 3. Additional quality flagging steps after flux processing. Flagged fluxes were assigned to quality class 2 if not in this class already according to the Mauder and Foken (2004) quality assessment. As CP time lag detection quality had been addressed earlier during flux processing in EddyPro, it was not screened at this stage.

	Applied to		# of flagged fluxes	
Step	OP fluxes	CP fluxes	OP	CP
1: Raw data skewness/kurtosis	yes	yes	23769 (23 %)	12043 (18 %)
2: Instrument signal stregth	yes	no	6951 (7 %)	n/a
3: Time lag detection quality	yes	no	20277 (20 %)	n/a
4: Abolute concentration limits	yes	yes	223 (0.2 %)	2261 (3 %)
5: Exclusion of outliers when simultaneous CP fluxes close to zero	yes	n/a	346 (0.3 %)	n/a
6: Absolute flux limits	yes	yes	634 (0.6 %)	102 (0.6 %)

Table 4. Estimates of scaling factor $\xi \pm 95$ % confidence intervals used for open-path flux correction. ξ describes the portion of the self-heating correction term, given by Burba et al. (2006) for vertically installed instruments, that is needed to correct OP fluxes determined with inclined gas analyzers. The scaling factor was optimized as a parameter of a nonlinear function where CP data were regarded as true fluxes. It was therefore determined for years when parallel CP and OP measurements were available. In case of an optimization converging to unreasonable values (below zero), we used the median of the remaining ξ estimates.

Year	Daytime ξ	Nighttime ξ
2010	0.0076 ± 0.0012	0.0071 ± 0.0013
2011	0.0116 ± 0.0009	0.0068 ± 0.0015
2013	0.0150 ± 0.0007	0.0104 ± 0.0009
2014	0.0094 ± 0.0006	0.0071
2015	0.0050 ± 0.0010	0.0071
2016	0.0051 ± 0.0005	0.0071
2017	0.0069 ± 0.0005	0.0071

Table 5. Spearman's rank correlation coefficient r_s and Pearson's correlation coefficient r between closed-path (CP) and open-path (OP) fluxes with and without the applied self-heating correction. The agreement between CP and OP fluxes increases throughout all quality classes after OP correction.

		Quality class 0	Quality classes 0,1	Quality classes 0, 1, 2
r_s	OP uncorrected	0.896	0.866	0.508
	OP corrected	0.907	0.871	0.512
r	OP uncorrected	0.894	0.871	0.042
	OP corrected	0.904	0.877	0.055

Table 6. Normalized mean contributions of the surface classes defined by Muster et al. (2012) to the eddy covariance footprint. Values were averaged over each subperiod and normalized to sum up to 1. Additionally, the mean non-normalized sum of all surface class contributions is given as column *Image contribution*. These values indicate how sufficient the classified area is to describe the EC footprint. Non-normalized half-hourly contributions of the single classes are given in the provided data set.

Year	**Tundra**		**Water**		**Median image**
	dry	***wet***	***overgrown***	***open***	**contribution**
2002	0.71	0.17	0.07	0.05	0.88
2003	0.70	0.17	0.07	0.05	0.87
2004	0.71	0.16	0.07	0.06	0.88
2005	0.71	0.17	0.07	0.05	0.87
2006	0.70	0.17	0.07	0.06	0.86
2007	0.54	0.37	0.06	0.02	0.73
2008	0.53	0.34	0.09	0.04	0.77
2009 I	0.54	0.32	0.08	0.06	0.72
2009 II	0.64	0.19	0.09	0.08	0.71
2010	0.65	0.18	0.09	0.08	0.73
2011	0.67	0.18	0.08	0.07	0.79
2012	0.67	0.18	0.08	0.07	0.80
2013	0.69	0.17	0.08	0.06	0.83
2014	0.66	0.18	0.08	0.07	0.77
2015	0.66	0.18	0.08	0.08	0.78
2016	0.65	0.18	0.09	0.08	0.74
2017	0.67	0.18	0.08	0.07	0.82

Table 7. Description of columns included in the data set file.

Column name	Unit/Format	Description
Date/Time (Local)	yyyy-mm-ddTHH:MM	Timestamp referring to end of 30 minute flux calculation period in local time (UTC+9h).
Date/Time (UTC)	yyyy-mm-ddTHH:MM	Timestamp referring to end of 30 minute flux calculation period in UTC.
CP CO_2 flux	$\mu mol\,m^{-2}\,s^{-1}$	Closed path CO_2 flux
QC CP CO_2 flux	dimensionless	Closed path CO_2 flux quality classes 0, 1 and 2
CP CO_2 flux rand unc	$\mu mol\,m^{-2}\,s^{-1}$	Closed path CO_2 flux random uncertainty estimate (Finkelstein and Sims, 2001)
OP CO_2 flux	$\mu mol\,m^{-2}\,s^{-1}$	Open path CO_2 flux
OP corr CO_2 flux	$\mu mol\,m^{-2}\,s^{-1}$	Corrected open-path CO_2 flux (Kittler et al., 2017)
QC OP CO_2 flux	dimensionless	Open path CO_2 flux quality classes 0,1 and 2
OP CO_2 flux rand unc	$\mu mol\,m^{-2}\,s^{-1}$	Open path CO_2 flux random uncertainty estimate (Finkelstein and Sims, 2001)
CO_2 flux comp	$\mu mol\,m^{-2}\,s^{-1}$	Time series compiled of open and closed-path quality class 0 and 1 fluxes
CO_2 flux gf	$\mu mol\,m^{-2}\,s^{-1}$	Gap filled Gap-filled CO_2 flux time series
QC CO_2 flux gf	dimensionless	Quality flag of gap-filled fluxes, between 0 and 3 (Reichstein et al., 2005)
CO_2 flux gf std	$\mu mol\,m^{-2}\,s^{-1}$	Standard deviation of gap-filled flux estimates, calculated from the data used for averaging
FP CC dry	dimensionless	Contribution of surface class *dry tundra* to the eddy covariance footprint
FP CC wet	dimensionless	Contribution of surface class *wet tundra* to the eddy covariance footprint
FP CC ove	dimensionless	Contribution of surface class *overgrown water* to the eddy covariance footprint
FP CC wat	dimensionless	Contribution of surface class *open water* to the eddy covariance footprint